PB85-221414

ICP-AES MULTIELEMENT ANALYSIS OF INDUSTRIAL HYGIENE AIR SAMPLES

By

R.D. Hull

50272-101

REPORT DOCUMENTATION PAGE	1. REPORT NO.	2.	3. Recipient's Accession No.

4. Title and Subtitle
ICP-AES Multielement Analysis Of Industrial Hygiene Air Samples

5. Report Date 85/01/16

6.

7. Author(s) Hull, R. D.

8. Performing Organization Rept. No.

9. Performing Organization Name and Address
Division of Physical Sciences and Engineering, NIOSH,
U.S. Department of Health and Human Services, Cincinnati, Ohio

10. Project/Task/Work Unit No.

11. Contract(C) or Grant(G) No.
(C)
(G)

12. Sponsoring Organization Name and Address
SAME AS BOX 9

13. Type of Report & Period Covered

14.

15. Supplementary Notes

16. Abstract (Limit: 200 words)

Inductively coupled plasma/atomic emission spectroscopy (AES) as a method for analyzing industrial hygiene air samples was evaluated. Low temperature oxygen plasma ashing and acid digestion procedures using nitric-acid or nitric-acid/perchloric-acid mixtures with samples containing 30 elements were investigated to determine the optimum technique for dissolving samples. Three different filters (cellulose ester, polyvinyl-chloride copolymer, and polycarbonate) were evaluated for trace metal contamination. Detection limits were determined using adjustable cross flow, fixed cross flow, or high solids nebulizers. Field samples were analyzed by AES and atomic absorption spectroscopy (AAS). Low temperature oxygen plasma ashing was faster than either acid digestion procedure. Polycarbonate filters had the lowest concentrations of contaminants. Cellulose ester filters were the easiest to ash or digest. Detection limits were lower for adjustable and fixed cross flow than for high solids nebulizers. Correlation between AES and AAS results of the field samples was generally good. Overall precision of the method was approximately 3 percent relative standard deviations. The author concludes that AES is a viable method for analyzing industrial hygiene air samples. The optimum procedure involves collection of samples on cellulose ester or polycarbonate filters, digestion by low temperature oxygen plasma ashing, and fixed cross flow nebulization.

17. Document Analysis a. Descriptors

b. Identifiers/Open-Ended Terms

NIOSH-Publication, NIOSH-Author, Plasma-membrane, Airborne-dusts, Quality-standards, Trace-metals, Airborne-particles, Spectroscopes, Quantitative-analysis, Polymers, Spectrographic-analysis

c. COSATI Field/Group

18. Availability Statement	19. Security Class (This Report)	21. No. of Pages 68
	20. Security Class (This Page)	22. Price

PB85-221414

Summary

The use of Inductively Coupled Plasma-Atomic Emission Spectroscopy (ICP-AES) for the analysis of industrial hygiene samples was evaluated. Experiments were conducted to define the lower limit of quantitation and the analytical range of each element for which an Occupational Safety and Health Administration personal exposure limit exists. The effects of varying the solution matrices and the concentrations of common elements such as sodium and potassium were determined. Interelement effects were also investigated.

Various acid digestion procedures were evaluated in conjunction with low temperature oxygen plasma ashing to determine the optimum technique for dissolution of industrial hygiene air samples. Three different filter materials (cellulose ester, PVC copolymer, and polycarbonate) were evaluated for trace metal content and lot-to-lot variability. Spiked filters and field samples were also collected and analyzed in the evaluation of this technique.

ICP-AES proved to be a viable technique for the multielement analysis of industrial hygiene personal air samples. The optimum procedure included collection on cellulose ester or polycarbonate filters and digestion by low temperature oxygen plasma ashing. Acid digestion was acceptable although it produced higher reagent blanks and required more time than the oxygen plasma ashing.

ICP-AES Multielement Analysis of Industrial Hygiene Air Samples

R. D. Hull

National Institute For Occupational Safety and Health
Division of Physical Sciences and Engineering
Methods Research Branch

January 16, 1985

DISCLAIMER

Mention of company names or products does not constitute endorsement by the National Institute for Occupational Safety and Health.

INTRODUCTION

The National Institute for Occupational Safety and Health (NIOSH) has the responsibility for research related to occupational health, including development and evaluation of analytical methods for determining hazardous workplace substances [Occupational Safety and Health Act of 1970 (PL91-596)]. The evaluation of workplace atmospheres that contain a variety of hazardous elements (Table I) requires sampling and analytical techniques which are capable of rapidly and simultaneously determining a large number of elements over a broad concentration range.

For elemental analysis, Inductively Coupled Plasma-Atomic Emission Spectroscopy (ICP-AES) appears to meet these requirements (rapid and multielement) whereas other techniques have failed. X-Ray fluorescence and conventional emission spectroscopy are not adequately sensitive for some elements of industrial hygiene importance. Although atomic fluorescence and flame and furnace atomic absorption spectroscopy usually have sufficient sensitivity, they are not multielement techniques. The poor precision of spark source mass spectrometry due to problems in sample vaporization makes this technique inadequate for exposure monitoring. Additionally, ICP-AES provides an analytical throughput considerably higher than these other techniques (Table II)(1).

ICP-AES involves the introduction of aerosols (created by nebulization of liquid samples) into an argon plasma. Atoms and ions that are generated from the sample species in the plasma are measured by observation of their characteristic emission spectra (1). The inherent physical properties of the plasma system offer performance and operational advantages over traditional arc and spark emission systems (2). The sensitivity and accuracy are very good and the range of applications is open-ended (3). Other performance characteristics of the ICP system include: a linear dynamic range over 4-5 orders of magnitude, a relatively clean background (primarily consisting of argon lines and weak band emission from OH, NO and CN molecules) which combined with a high signal-to-background ratio of analyte emission gives low detection limits, minimal matrix interference, and remarkable stability over long periods of operation (3).

The purpose of this work was to develop in-house capabilities for ICP-AES multielement analyses of industrial hygiene (air) samples. The protocol for achieving this objective included: (a) verifying a lower quantitative limit for analysis of samples (a low concentration limit at which precision and accuracy are acceptable for analysis of samples) for all hardwired channels and for those elements that are not hardwired but for which an Occupational Safety and Health-Permissible Exposure Limit (OSH-PEL) exists; (b) investigating ways to improve precision and accuracy of the analytical system; (c) determining optimum filter matrix, dissolution procedure and solution matrix for collection and analysis of air samples; and (d) verifying the applicability of the sampling and analytical methodology developed by analysis of spiked and field samples.

EXPERIMENTAL

Apparatus

The ICP-AES system employed for this study was a Jarrell Ash Model 1160 Plasma Atomcomp with a Digital Equipment Corp. Model 11/34 computer and Plasma Therm Model HFP2000D Radio Frequency (R.F.) generator. The system has 32 hardwired channels (Table III) and one variable channel (n+1 monochromator). A schematic of the system and technical specifications are shown (Figure 1 and Table IV, respectively). Reference solutions were prepared by dilution of 1000-µg/mL stock solutions (ICP grade) purchased from SPEX Industries. High purity reagents (HNO_3 - Suprapur, Matheson Coleman and Bell and Ultrex , J. T. Baker; $HClO_4$ - double distilled, G. Frederick Smith Chemical Co.; H_2SO_4 electronic grade, E. I. duPont de Nemours & Company; H_2O_2 - Sargent Welch Scientific) and deionized, distilled water (distilled following treatment with a Millipore Super-Q system) were used.

Optimization of Analytical Parameters

Optimum plasma operating conditions (R. F. generator power, observation height and sample uptake rate) vary for different elements due to their differing spectro-chemical properties.(4) That is, an easily ionized element (e.g. sodium) is determined using an atomic line in the visible region of the spectrum (589.0 nm) while an element like cadmium is determined at its ionic line in the ultraviolet region of the spectrum (226.5 nm). These lines are used since they are the most sensitive emission lines for these elements.

Plasma operating conditions cannot be fully optimized for each of these elements simultaneously since the high temperature that is required to ionize cadmium and produce intense ionic emission (optimum detection limit) will also cause considerable ionization of sodium and consequently a low atomic population will be available. A cooler plasma will favor sodium atomic emission but will not have as much energy available to ionize cadmium as the hotter plasma. Consequently, for analysis of a wide range of elements it is necessary to operate the plasma at compromise conditions; however, there are compromise conditions under which the extent of ionization and detection power are balanced so that simultaneous multielement analysis is practical (4). Optimization of these parameters is typically accomplished by maximizing the intensity ratio of a dilute solution (~1 μg/mL of Cd or Zn) and a blank solution by varying (in the following order) RF power, observation height and sample uptake rate (5). Optimization of variables was conducted by this procedure for three different nebulizer designs [adjustable cross-flow, fixed cross-flow and high solids (Fig. 3)]. The detection limits, precision, sensitivity (slope of calibration curve), and background equivalent concentration (intercept of calibration curve) were also determined. A simplex optimization of variables (6) was investigated as an alternative to the previously described procedure.

Interferences

Analyte species are subjected to relatively high temperatures (5000 - 8000^{o}K), long residence times (~2 msec) and an inert environment in the plasma. These factors combine to eliminate, or at least minimize most chemical or matrix intereference effects that are found in many flames, arc, and spark discharges (7). Some interferences do exist however and can be grouped into three categories.

Physical interferences or "nebulization and transport effects" (8,9, 10) are the influences that determine the rate and form (i.e. particle size) in which analytes are delivered to the plasma. Changes in density and viscosity of different acids and acid concentrations affect the sample uptake rate. These effects are generally minimized by matching the acid concentrations of samples and standards and using a peristaltic pump to provide a uniform sample flow. The magnitude of these effects was determined by comparing the precision, correlation coefficients, slope and intercept of standards prepared in different acid matrices (HNO_3, $HNO_3/HClO_4$ and H_2SO_4/H_2O_2). The effect of a peristaltic pump (Gilson model HPIS) for sample delivery to the nebulizer on intensity, precision and detection limits was also evaluated as was the effect of humidifying the argon used for nebulization.

Chemical interferences (2, 7, 8, 9) are characterized by molecular compound formation, ionization effects and solute volatilization effects. These effects are not severe in ICP analysis and are minimized by careful selection of operating conditions (incident power, sample uptake rate and observation height). Matrix matching or buffering the sample may also be used to minimize this type of interference. Investigations of classical solute volatilization interferences [Ca–PO_4 and Ca–Al systems which form refractory compounds, $Ca_2P_2O_7$, $Ca_{3-}(PO_4)_2$, $Ca_3Al_2O_6$ etc.] revealed an absence of any depression in intensity for low molar ratios and only a very slight suppression in intensity for PO_4^{3-}/Ca^{+2} molar ratios up to 1000 and Al^{+3}/Ca^{+2} molar ratios up to 100 at an observation height of 20 mm above the work coil (9). Since this work (solute volatilization interference) is well documented (7) and interferences are shown not to exist

at low molar ratios and only be minimal at high ratios, additional work was not conducted in this area. Interference effects produced by easily ionizable elements were investigated by comparing intensities obtained for 10-µg/mL solutions of aluminum, cadmium, lithium, nickel and thallium that were 0.0, 1.0, 5.0 and 10.0% (w/v) NaCl.

Spectral interferences (8,11) include (a) unresolved overlap of molecular band spectra, (b) overlap of a spectral line from another element, (c) background from continuous or recombination phenomena and (d) background from stray light. The first effect (overlap of molecular band spectra) was minimized by judicious line selection (Table III). The other types of spectral interference (spectral overlap and elevated background) were investigated. Single element standards of 10, 100 or 1000-µg/mL were aspirated and the intensity observed by each photomultiplier recorded. A spectral scan ($\pm$ 1Å) was then conducted at each wavelength which exhibited an intensity increase and the determination made as to whether the interference was due to spectral overlap, elevated background or contamination of the standard. Sodium and potassium were investigated in addition to each of the elements which are hardwired into the system.

Correction for interelement interferences (spectral line overlap and elevated background) was achieved with our instrument by measuring the effect of the interfering element A on element B using a pure reference solution. A factor K_{BA} was obtained from this measurement which, when multiplied by the actual

concentration of A (C_A actual) determined during sample analysis, gave a correction factor which was subtracted from the observed concentration of B(C_B observed) (13):

$$C_B \text{ corrected} = C_B \text{ observed} - K_{BA}C_A \text{ actual.}$$

The problem was compounded (for some elements) by the fact that more than one element had spectral interference on element B. Therefore, the correction on C_B observed must include the sum of all of the concentration corrections:

$$C_B \text{ corrected} = C_B \text{ observed} - \sum_j K_{Bj}C_j \text{ actual.}$$

This procedure was followed for every determination affected by interelement spectral interference (computations done by the computer after entering in the K factors).

Quality Assurance

Several quality control measures were utilized for this study. A log book was maintained in which the "on time" and instrument adjustments and repairs were recorded. Also recorded were the mercury profile settings, copper/manganese intensity ratios and slope and intercept of calibration curves.

The mercury profile setting was obtained by rotating the micrometer mounted quartz refractor plate [behind the entrance slit (Fig. 1)] to achieve the

maximum intensity of the mercury line at 435.8 nm. Rotation of the refractor plate causes the radiation to be shifted either right or left so that the peak can be maximized on the exit slit (and consequently the photomultiplier). The mercury source is a pen ray lamp located immediately in front of the entrance slit which can be rotated into or out of the optical path. Profiling in this manner (at the beginning of each day and after every four hours of operation) assures that slight deviations which result from changes in the refractive index of air, are corrected.

The interelement interference (spectral line overlap) correction factors (K) are affected by variations in the analysis region excitation temperature of the plasma. These temperature variations are due to the day-to-day variations in the aerosol carrier flow-rate. Botto (12) devised a procedure for assuring the reproducibility of the plasma temperature and consequently the interelement correction factors. This procedure involves measuring the Cu/Mn intensity ratio (for a 10-μg/mL mixed element standard) and adjusting it to fall within a certain range (one standard deviation of ten consecutive intensity measurements - performed immediately after optimizing the instrumental operating parameters). The Cu/Mn intensity ratio was adjusted by changing the pressure regulator for the carrier argon. A new Cu/Mn ratio was determined whenever modifications or adjustments were made to the instrument.

The slope and intercept of the calibration curves were obtained by computer printout following standardization. Any significant deviations (in either slope or intercept) from previously determined values, necessitated restandardization.

Standardization and Quantitative Limits

The ICP-AES instrumental analytical system utilizes a two point standardization. The computer determines a line (calibration curve) from the intensity ratios of two measurements (typically an acid blank and a 10-µg/mL reference solution) for each element. The linearity of these calibration curves was investigated (for all hardwired elements) by analyzing several standard solutions bracketing the range of approximately 5 to 10 times the calculated detection limit (2 times the signal to noise ratio) to 10 µg/mL. The calculated detection limit is determined by the computer as 2 times the signal to noise ratio. A low quantitative limit for analysis and the precision at this limit were also determined as were the precision and stability (over a 4-h period) at 10 µg/mL. Additionally, since a maximum of 7 standard solutions (software limited by Jarrell-Ash) may be used for standardization, it was necessary to determine if contaminants existed in the reference solutions and the compatability of the different metal species.

Analysis parameters (wavelength, slit widths, aperture and dynode settings) were determined on the variable wavelength channel (n+1 monochromator) for five additional elements of industrial hygiene importance (Ba, Hf, Rh, Sb and Ta). The same analytical parameters determined for the hardwired channels were also determined for these five elements and the interference (if any) caused by these elements on the 32 hardwired channels determined.

Development of Sampling and Analytical Methodologies

The collection of particulates by filter/vacuum pump sampling is used extensively for industrial hygiene monitoring (14). Several different filter media may be employed based on the sampling requirements and the analytical technique. For analysis by ICP-AES, the optimum collection media would exhibit (a) low metal background contamination, (b) ease of dissolution, and (c) a final solution matrix conducive to optimum detection limits, precision and accuracy.

Three different filter materials were investigated. Cellulose ester filtersfrom Millipore Corp. (37mm, 0.8-μm pore size, type AA Lot numbers 31076-4 and C7M21891), PVC-copolymer filters from Gelman Sciences, Inc. (37-mm, 0.8 μm pore size, type DM800, Lot numbers 81867 and 2595099) and polycarbonate filters from Nuclepore Corp. (37-mm, 0.4 μm pore size, Lot numbers 73B8345 and 81F7A37). Two lots were obtained from each supplier so that an estimate of lot-to-lot variability could be obtained. Three sets of six filters each and two blanks were acid or low temperature oxygen plasma (International Plasma Corp., Model 4000) ashed for each lot of filter material. A detailed description of the ashing procedures is listed in Table V. Briefly, the cellulose ester filters were ashed in HNO_3 or the low temperature oxygen plasma asher (LTA) and the residue dissolved in HNO_3 and diluted to volume (5 mL), the PVC-copolymer filters were ashed in a mixture of $HNO_3/HClO_4$ or the LTA and the residue dissolved in $HNO_3/HClO_4$ and diluted to volume (5 mL), and the polycarbonate filters were ashed in a mixture of H_2SO_4/H_2O_2 or the LTA and the residue dissolved in

H_2SO_4/H_2O_2 and diluted to volume (5 mL). Standards were prepared in an acid matrix to match the filter samples.

The background metal concentrations were determined for each filter set and the ease of digestion, detection limits, precision and accuracy determined for the different matrices.

Application of Sampling and Analytical Methodologies

The optimum analytical methodologies were tested by digesting and analyzing spiked filter samples as well as field samples collected from: (a) welding and brazing atmospheres, (b) alloying plant atmospheres and (c) plating operations atmospheres.

Cellulose ester filters were spiked at 2.50-µg metal/filter and 1000-µg metal/filter. Multielement spikes (Table XVIII) were used. Digestion of the filters was accomplished with either $HNO_3/HClO_4$ (5 mL of 5:1 HNO_3:$HClO_4$ for 6 hours @ 120°C) or HNO_3 (10 mL for 18 hours @ 120°C). A final acid concentration of 5% and solution volume of 10 mL was used. Low temperature ashing was attempted; however, of the three LTA's available, none were operating or could be made operational. Silicon and boron were not determined since the digestions were conducted in glassware (Teflonware is necessary for Si and B determinations).

Field samples were collected at ~2.0 L/min using a Lippman-type sampler (Fig. 2) in an attempt to achieve sample homogeneity. The samples were digested by either acid or low temperature oxygen plasma ashing. Both atomic absorption and ICP-AES analyses were conducted for several of the metals.

RESULTS AND DISCUSSION

Nebulizer Evaluations

The three different nebulizer designs shown in Figure 3 were investigated (adjustable cross-flow, fixed cross-flow and high solids). The adjustable cross-flow nebulizer was received with the instrument but in early experimentation exhibited several shortcomings. The glass sample needle often plugged and on several occasions either broke or was knocked out of alignment as attempts were made to clear it. Additionally, alignment of the needles was done external to the instrument (this was necessary as the needles had to be observed under magnification to insure that they did not contact each other and break) and it was found on several occasions that when the nebulizer was returned to the spray chamber, the nebulizer housing was sufficiently distorted (due to the tight fit over the spray chamber) to render it out of alignment. Consequently, when these other two nebulizer designs were made available, they were investigated as replacements.

The fixed cross-flow nebulizer was designed to overcome several of the problems associated with the adjustable cross-flow nebulizer. The fragile glass needles were replaced with a sapphire orifice for the argon gas and a platinum/iridium needle for the sample. Alignment would not be a problem

since the nebulizer is has no adjustable components. Clogging was also expected to be less of a problem since the Pt/Ir needle had a straight bore, unlike the tapered bore of the glass needle (due to the glass being heated and "drawn" to a fine tip). Provided this nebulizer exhibits acceptable precision, sensitivity and detection limits and works as expected, its replacement of the adjustable cross-flow nebulizer would be a significant improvement in the analytical system.

The high solids nebulizer was developed (15) for the nebulization of samples with high salt content. These types of samples are difficult to analyze with a conventional nebulizer as an appreciable salt build-up on the needles occurs which significantly reduces the analytical precision. Although industrial hygiene samples collected in air are unlikely to require this high solids nebulizer for analysis, it may prove beneficial for the analysis of bulk samples, urines and blood plasmas. For this reason and the fact that it could be used for the analysis of routine samples (provided its performance characteristics were adequate) this nebulizer was also evaluated.

The optimum plasma operating conditions (R.F. power, observation height, nebulizer argon pressure and sample uptake rate) are listed in Table VI for the three nebulizer types. These optimal conditions were determined sequentially as outlined in the experimental section.

The simplex optimization of variables (6) allows for the optimization of interrelated, continuously variable parameters. Since the R.F. power,

observation height and sample uptake rate are interrelated it was thought the simplex procedure might result in a "truer" optimization. A simplex optimization of variables was conducted on the fixed cross-flow nebulizer and gave results identical to those determined univariately. Additionally, the simplex procedure did not reduce the time required for optimization but instead required longer to accomplish. For these reasons, the sequential optimization of parameters was utilized for all additional studies.

Detection limits for the three nebulizers are compared in Table VII. In general, the detection limits for the adjustable cross-flow and fixed cross-flow nebulizers were quite similar while detection limits for the high solids nebulizer were approximately a factor of two poorer.

The precision (Table VIII) of blank solutions was very similar for all three nebulizers (0.41-3.46, 0.44-2.30 and 0.32-2.06% RSD for the adjustable, fixed and high solids nebulizers, respectively) as was the precision for 10-μg/mL standards (0.28-2.83, 0.58-6.02 and 0.54-7.79% RSD for the adjustable, fixed and high solids nebulizers, respectively). The long term precision (1-10 sec burn every 1/2 hour over a four hour period) was considerably poorer (by a factor of ~3) for the high solids nebulizer (8.6-16.0% RSD) than the fixed cross-flow nebulizer (2.5-5.3% RSD) and the adjustable cross-flow nebulizer (1.2-6.0% RSD).

The sensitivities (slope of the calibration curve) and background equivalent

concentrations (intercept of the calibration curve) obtained with the three nebulizers are listed in Table VIX. The fixed cross-flow nebulizer is approximately twice as sensitive as the high solids nebulizer [0.097-2.37 vs. 0.046-0.742 intensity ratio (μg/mL)]. The adjustable cross flow nebulizer is approximately midway between the other two nebulizers in sensitivity [0.023-1.55 intensity ratio/(μg/mL)]. The background equivalent concentration is a measure of the signal-to-background ratio and is therefore one of the most important specifications. The background equivalent concentrations were best for the fixed cross-flow nebulizer (0.013-2.39-μg/mL), poorer for the adjustable cross-flow nebulizer (0.023-2.59-μg/mL) and poorest for the high solids nebulizer (0.029-5.17-μg/mL).

One additional factor (reliability) should also be considered in comparing the different nebulizers. The adjustable cross-flow nebulizer clogged several times during sample analysis. Approximately 50% of the time the nebulizer could be cleared by syringe injection of distilled water into the sample uptake tube. If this failed to restore operation, then a cleaning wire was inserted into the sample uptake tube and through the sample needle of the nebulizer. In performing these repairs, the nebulizer was often knocked out of alignment or one of the fragile glass needles broken. Consequently, when using the adjustable cross-flow nebulizer approximately 15% of the operators time was spent in nebulizer repairs or adjustments. The high solids nebulizer never plugged or caused operational problems of

this type. The fixed cross-flow nebulizer did plug occasionally but was always easily remedied with a syringe injection of distilled water.

In general, the adjustable cross-flow and fixed cross-flow nebulizers compared favorably while the high solids nebulizer exhibited poorer performance parameters in nearly all respects. Due to the significantly greater ease in operation of the fixed cross-flow nebulizer, it was used in the subsequent experiments.

Interferences

Physical interferences were investigated by comparing the precision slopes and intercepts obtained from standards (0.1- 10-µg/mL) prepared in different acid matrices (5% w/v HNO_3, 5% w/v HNO_3/5% w/v $HClO_4$ and 5% w/v H_2SO_4/2% w/v H_2O_2) (Table X). The correlation coefficients are not listed since they were better than 0.999 for each metal in each acid matrix. The sensitivities (slope of calibration curves), background equivalent concentrations (intercept of calibration curve) and precisions were very comparable. However, general trends in the data indicate that each one of the matrices (HNO_3, HNO_3/$HClO_4$ and H_2SO_4/H_2O_2) produces optimal performance characteristics (sensitivity, background equivalent concentration or precision). Seventy precent of the elements exhibited optimal sensitivity in HNO_3, 23% in HNO_3/$HClO_4$ and 7% in H_2SO_4/H_2O_2. Fifty percent of the elements exhibited the best background equivalent

:entrations in H_2SO_4/H_2O_2, 45% in HNO_3 and only 5% in $HNO_3/HClO_4$. The best precisions were determined in $HNO_3/HClO_4$ (60% of the elements), followed by HNO_3 (30% of the elements) and then H_2SO_4/H_2O_2 (10% of the elements). Table X is included since the trends noted above are generalizations and may not hold true for every element. The performance characteristics of all of these 31 elements in each of these three matrices are listed in this table.

The results from using a peristaltic pump to maintain controlled delivery of sample to the nebulizer are shown in Table XI. When using the pump the intensity of a blank solution was lower and the difference in intensity between a 10-μg/mL standard and a blank was greater than when the pump was not used. Also, the short term precision was better when the pump was used. These advantages of using the pump were balanced by the fact that the detection limits were better (by a factor of two) when the pump was not used. Use of the pump also eliminated the occasional clogged nebulizer needle. These advantages (larger intensity difference between blank and standard solutions improved precision and reduction in clogged nebulizer problems) outweighted the disadvantage (poorer detection limits); consequently, the pump was used in the remaining experimentation.

One recommendation of another plasma emission spectroscopist (Dr. Roy Kuennen, April 17, 1980) was that humidification of the nebulizer argon

significantly improved the analytical precision and also helped prevent salt build-up on the nebulizer needle (for high salts samples).

This was investigated by comparing the intensities and precision obtained for a blank (5% HNO_3) solution and a 10-µg/mL multielement solution of Al, Cd, Li, Ni and Tl analyzed both with and without humidification. Two brass bubblers (each containing 50 mL distilled deionized water) were placed in series and connected to the nebulizer argon line. A two-way valve was placed upstream of the bubblers so that it was easy to switch to or from humidification of the argon without having to turn off the plasma. Table XII lists the data from this experiment. The precision of the acid blank was better without humidification; however, the precision at 10 µg/mL was better with humidification. Humidification also tended to lower the intensity of the acid blank and the 10-µg/mL standard (except of lithium where the intensity at 10 µg/mL was greater with humidification). Consequently, these experiments indicated the effects produced by nebulizer argon humidification were not sufficiently advantageous to be used routinely.

An additional experiment evaluated the effect of argon humidification on samples with a high salt content (1, 5 and 10% w/v NaCl) and the effect of a high concentration of an easily ionizable element on other elements. Multielement samples (in 5% HNO_3) that were 10-µg/mL each in Al, Cd, Li, Ni and Tl were also made 0, 1, 5 or 10% w/v in NaCl. These samples were analyzed both with and without humidification of the nebulizer argon and the

absolute intensities and precision recorded (Table XIII). The data show that the precision is considerably better with high salt contents when nebulizer argon humidification is employed; however, the effects of large quantities of easily ionizable elements (Na in particular) must be compensated for by matrix matching. Samples that were 10% w/v NaCl caused a decrease in intensity of ~15% for a 10μg-Al/mL solution, ~20% for a 10-μg Cd/mL solution, and ~30% for 10-μgNi/mL and 10-μg Tl/mL solutions. Lithium intensities increased upon the addition of NaCl. It is not certain whether the NaCl was contaminated with lithium or if the excess of electrons furnished by the ionization of sodium caused a lesser degree of ionization by lithium and consequently a higher number of transitions originating from the atomic state (lithium is monitored at 670.78 nm - an atomic line). Based on these results, samples that have very high salt contents (some bulk samples and samples digested by fusion) should be analyzed by matrix matching and argon humidification. Typical samples (industrial hygiene samples collected from air) do not require humidification or matrix matching (other than the acid content).

Spectral interferences were determined by aspirating 10, 100 or 1000-μg/mL single element standards and observing the response for each channel. Each channel giving a response was "scanned" (±1.0Å) and a plot obtained from which it was determined in conjunction with wavelength tables (15, 16) whether the intensity increase was due to spectral overlap, elevated

_____ground or contamination of the standard. The scanning ability of the system is demonstrated in Figure 4 which shows the beryllium peaks at 3130.4Å and 3131.1Å. Table XIV provides a breakdown of the results of this experiment. Although several elements exhibited more than one type of interference on other channels, some generalizations can be made. Aluminum elevates the background for several elements while tungsten interferes with several elements. Molybdenum produces both elevated backgrounds and interelement interferences. Arsenic, lithium, phosphorus, selenium and thallium did not cause interferences on the other channels. Several standards were contaminated with sodium. The aluminum elevated background effect on arsenic is shown in Figure 5. As additional aluminum is added, the baseline increases. At 1000 µgAl/mL the baseline produces approximately twice the intensity of a 10-µgAs/mL standard determined with no aluminum present. Similarly, the spectral overlap of iron on platinum is shown in Figure 6. As can be seen, a 1000-µg Fe/mL solution gives the same response as 10-µg Pt/mL. The worst case of spectral overlap observed with our instrument is shown in Figure 7. Platinum and tungsten both give a response on the arsenic channel. A 10-µg Pt/mL solution creates an apparent arsenic concentration of 5-µg/mL. The tungsten interference is not as severe since the tungsten peak is offset further from the arsenic peak. Correction for these interferences was accomplished by determining the K factors and programming these into the computer. The K factor was obtained by analyzing a single element reference solution (100 or 1000-µg/mL) and observing the apparent concentration registered on channels other than that of the

analyte. The K factor is the result of dividing the apparent concentration (interference) by the actual concentration being analyzed. For example, when a 100-µg/mL solution of iron is aspirated, an apparent concentration (interelement interference) of 0.43-µg/mL is observed on the arsenic channel; therefore:

$$K = \frac{0.43}{100} = 0.0043$$

A list of the K factors and the associated elements and channels are given in Table XV. A total of 53 interelement corrections (K factors) are used and have been programmed in the computer for automatic correction of sample results.

Quality Assurance

The three operational parameters associated with quality assurance (mercury profile settings, plasma temperature and calibration curves) are checked daily and adjusted if necessary before analyses are conducted.

The mercury profile setting typically varies from 670-700 (micrometer settings). When the intensity of the mercury line drops to 80% or less than its original value (when the instrument was new), the entrance slit is removed from the spectrometer and cleaned. The entrance slit is the only unsealed opening into the spectrometer and must be cleaned occasionally (approximately once every eight months).

Maintaining a constant plasma temperature on a day-to-day basis (which is necessary for use with correction factors) is conducted by determining the

Cu/Mn intensity ratio and adjusting it (by changing the nebulizer argon pressure) to fall within a preset range. This range is plus or minus one standard deviation of the average of ten consecutive Cu/Mn determinations (performed after any repair or modification of the instrument and subsequent optimization of analytical parameters). A typical average and standard deviation of the Cu/Mn ratio was 0.7124 and 0.0040, respectively. The Cu/Mn intensity average has varied from 0.6967 to 0.7645 depending on the nebulizer and torch used.

Following standardization, the slopes and intercepts of the calibration curves were listed and compared to previously determined values (Table XVI). Differences of greater than 10% indicated improper standardization or a system malfunction and were corrected by either restandardization or repair of the instrument.

Quality control samples (spiked filters) were analyzed in conjunction with field samples and are discussed in that section of the report (Application of Sampling and Analytical Methodologies).

Standardization and Quantitative Limits

Calibration curves over the range of approximately 5 times the calculated detection limit to 10-μg/mL exhibited excellent linearity (correlation coefficients were better than 0.9999 in all cases) consequently plots of these curves were not reproduced. The verified lower quantitative limits for

analysis of samples, precision at these limits, precision at 10-µg/mL and the long term stability are listed in Table XVII. For all elements (excluding Carbon) the verfied lower quantitative limit was between 10 and 100-ng/mL with the precision (3 runs at 5 burns/run) at this level between 0.26 (yttrium) and 1.74% RSD (selenium). The precision (3 runs at 5 burns/run) at 10-µg metal/mL ranged from 0.28 (tin) to 2.83% RSD (lithium). The stability (change in response over a four-hour period for a 10-µg/mL solution) varied from an increase in response of 2.7% for arsenic to a decrease in response of 4.2% for nickel. The stability of 25% of the elements was less than or equal to one times the precision (% RSD) for that element at 10-µg metal/mL. Seventy-five percent of the elements exhibited stabilities better than or equal to two times the precision of that element at 10-µg/mL.

All channels except carbon exhibited excellent precision over the entire calibration range (better than 3.0% at both the upper and lower limits). The pooled precision (3 runs @ 5 burns/run) for determination with the carbon channel was 19.6, 19.3, 17.0, 17.4 and 14.5% RSD for distilled water and standards of 0.5-µg C/mL, 1.0-µg C/mL, 10-µg C/mL and 100-µg C/mL, respectively. The precision could not be determined at 1000-µg C/mL since determinations at this level were off scale. The change in response (over a four-hour period) for a 10-µg C/mL solution was 42%. This channel was decidedly not quantitative and was not used further for analysis.

Because of absolute linearity, standardization only involves determining the intensities of a blank solution and the intensity of 10-µg/mL standards (calibration curves are defined by the lines passing through these points). Since a maximum of seven standard solutions (software limited by Jarrell-Ash) may be used for standardization (and one of these is the "blank") multielement standards are necessary. More than one multielement standard is necessary due to chemical incompatability (chromates, vanadates formation, etc.) interelement inference and contaminants in the standards. After comparing the interelement interferences, concomitants in the reference solutions (Table XIV) and the chemical compatibilities, the configuration shown in Table XVII was determined the optimum pairings for the multielement standards.

The variable wavelength channel (n+1 monochromator) was investigated for its ability to quantitatively analyze other elements for which an Occupational Safety and Health Permissible Exposure Limit exists but which are not hardwired into our instrument. The optimum instrumental parameters (wavelength, slit settings and gain) are listed (Table XIX) as are several of the performance characteristics (lower quantitative limits, precision at these limits and at 10 µg/mL, stability and interferences).

Comparison of Different Filter Materials

The concentrations of metals determined in cellulose ester filters are listed in Table XX. All hardwired channels except carbon, boron and silicon were utilized for these experiments. Carbon was previously determined not quantitative and boron and silicon contamination was introduced by the glassware. Two "lots" (080577A05 and 080577A06) of cellulose ester filters

advertised specifically for trace metal collection and analysis were analyzed in addition tc the two lots of each of the three filter types (cellulose ester, PVC-copolymer and polycarbonate). These filters (specifically for trace metal analysis) had lower levels of calcium, copper, magnesium, manganese and sodium than the other cellulose ester filters. However, the concentrations of the other elements (aluminum, chromium, iron, nickel, phosphorus and zinc) were as high or higher than the other cellulose ester filters. Similar results were recorded whether low temperature or acid ashing was conducted. Additionally, lot-to-lot variations were minimal for nickel (all determinations were 0.005 or 0.006-μgNi/filters) but were large (>50% difference) for the other elements.

The PVC-copolymer filters contained the greatest number and highest levels of metals contamination as well as the largest lot-to-lot variability (Table XXI). The polycarbonate filters had very low levels of contamination and were consequently the "cleanest" of the three filter types investigated (Table XXI). For both Tables (XX and XXI) the absence of a number reported indicates contamination was below the detection limit for that element (the detection limits in Table XX also apply to Table XXI). Also, the detection limits used in this experiment are lower than the lower quantitative limits listed in Table XVII since the lower limits apply to the normal two-point standardization and that was not used for this experiment (a separate trace level calibration curve was prepared for each element).

Metal concentrations in any of the three filter media were not sufficiently high to preclude their use for typical industrial hygiene compliance monitoring. For industrial hygiene surveys where airborne metal concentrations

may be quite low, it is advisable to avoid the use of PVC-copolymer filters. There are, however, other considerations in addition to trace metal contamination when selecting a suitable filter material. The PVC-copolymer filters were considerally more difficult to ash than the other filters and the sulfuric acid matrix of the polycarbonate filters was previously determined not to be the optimum matrix for analysis with the cross-flow nebulizer (Table X).

A comparison of reagent blanks obtained from (a) low temperature plasma ashing/ultrapure HNO_3 dissolution; (b) ultrapure HNO_3 digestion and dissolution (two "lots" of acid) and (c) ACS reagent grade HNO_3 digestion/dissolution are listed in Table XXII. Concentrations of elements not listed were less than the detection limits shown in Table XX. Low temperature ashing is advantageous in that it exhibits considerably lower blank values than the acid digestions. Similarly, ultrapure acid exhibits significantly lower blank values than does ACS reagent grade acid.

Spiked Filters

Recoveries from the spiked filters are shown in Table XXIII. At high loadings (1000-µg metal/filter) $HNO_3/HClO_4$ appears to give better recoveries than HNO_3 alone; however, some metals (Be, Mo, P, Sn, and W) gave unsatisfactory recoveries with both acid digestions. At low filter loadings (2.5-µg metal/filter) neither digestion procedure ($HNO_3/HClO_4$ or HNO_3) appears to offer significant advantages (in terms of recoveries) over the other. Sodium and phosphorus background levels (from the acids) were too high to allow quantitative determination at these low levels. Five metals (Se, Sn W, Ti and Zr) exhibited poor recoveries (<90%) using the HNO_3 digestion. Three of

the same metals (Sn, W and Zr) in addition to lithium and manganese exhibited less than adequate (90% or better) recoveries for the HNO_3)/$HClO_4$ digestion.

Field Samples

Welding and brazing samples were collected on cellulose ester filters and digested in HNO_3 prior to analysis by ICP-AES and atomic absorption spectroscopy (AAS) (Table XXIV). Analysis was conducted by AAS in addition to ICP-AES since it is currently used extensively for the analysis of metallic industrial hygiene samples (viz. Reference 14, P&CAM 173). Correlation between the two techniques was good although the ICP-AES values were higher than the AAS values at the lower concentration levels (<~5-µg metals/filter). Standards were prepared from spiked filters therefore separate quality assurance samples (spiked filters) were not analyzed.

Ten samples (two "Lippman-type" samplers, each containing 5 sampling filters) were collected at a nickel alloying facility. The Lippman-type samples were used to try to obtain good homogeniety among the filter samplers so that a comparison of ashing techniques could be conducted on field samples. ICP-AES and AAS analyses were conducted on all of the samples. One-half of the samples from each sampler were acid digested (HNO_3/$HClO_4$) while the remaining samples were ashedted in the LTA. Correlation between the two analysis techniques is very good as there is no significant difference between the means for the two techniques. Recoveries appear to be higher for the acid-digested samples than those treated in the LTA. However, this is believed to be an anomaly of the low number of samples collected (due to breakdown of

process equipment at the primary sampling site) and the fact that the grinding operations sprayed some non-respirable particulate material into the samplers (which perturbed the homogeneity in the samplers). The lower recoveries from the LTA-treated samples could also be due to allowing insufficient time for solubilization of the metals after ashing (15 minutes at 120 °C was used). Quantitative recoveries from the quality assurance samples were obtained for both ashing procedures.

Table XXVI demonstrates one of the main advantages of LTA, which is the low blank values that are obtained. An advantage of ICP-AES over AAS is also shown in Table XXVI. The metals were quantitatively determined at the same time and from the same samples as those shown in Table XXV. Analyses for all of the metals by AAS would have been very time-consuming and would have necessitated a larger solution volume (consequently a longer sampling time) for analysis.

Seven samples (in one "Lippman-type" sampler) were collected at a chromium and nickel plating facility. Since the LTA was not working at this time, one-half of the samples were ashed in a $HNO_3/HClO_4$ mixture and the remaining samples ashed in HNO_3 alone. Correlation between the two analysis techniques (ICP-AES and AAS) is very good (Table XXVII). There is no significant difference between the means for the two techniques. Precision is quite comparable for the area samples; however, accuracy and precision of the quality assurance samples appears to be slightly better with ICP-AES analysis. Ashing with a mixture of nitric and perchloric acids or with nitric acid alone worked equally well for these samples. Also, as with the previous samples, additional metals (Al, Fe and Zn) were quantitatively determined (simultaneously with the

Ni and Cr) during the ICP-AES analysis. Sample-to-sample variability was less for these samples than the alloying plant samples; however, the variability was still sufficiently high to indicate that the sampler used does not provide a homogeneous distribution for particulates.

CONCLUSIONS

ICP-AES has been demonstrated to be a viable technique for analysis of industrial hygiene air samples. Various analytical parameters including precision, accuracy, range, and limitations (different types of interferences) are discussed in addition to investigation of optimum collection media and digestion/dissolution procedures. The analytical precision was determined to be better than 3% RSD and the analytical range quite broad. Interferences were found to exist, however; they were easily compensated for by using the appropriate techniques.

Spiked filters of 2.5 μg metal/fiter and 1000 μg metal/filter (0.25 and 100 μg metal/mL following digestion and dissolution) were ashed and analyzed with quantitative recoveries determined for most of the metals at both loading levels. Analysis of field samples (welding and brazing samples, alloying plant samples and plating plant samples was conducted by both ICP-AES and an established technique (AAS) with the results from the two techniques being quite comparable. ICP-AES also proved to be considerably less time-consuming for the analysis of multielement samples than AAS.

Specific conclusions are:

1. Both HNO_3 and $HNO_3/HClO_4$ are acceptable for sample digestion. Low temperature oxygen plasma ashing may be used for ashing of the filter matrix.

2. Preferred acid matrix for analysis is HNO_3 however $HNO_3/HClO_4$ is acceptable.

3. For routine sample analysis, a peristaltic pump should be used for sample delivery to the nebulizer as it improves precision and helps minimize nebulizer clogging.

4. The fixed cross-flow nebulizer should be used for routine analyses.

5. Cellulose ester is the optimum filter matrix due to its ease of ashing and the ashing/dissolution acids used with it are the most amenable to optimum sensitivity and precision.

6. Quality assurance samples (spiked filters) must be digested and analyzed with the samples (this is a good laboratory practice for all sampling and analysis procedures).

7. The digestion/dissolution procedure must be modified for certain elements (Li, Mn, Mo, P, Sn, W. Zr) (Reference 14 contains specific digestion/dissolution procedures for most of these elements).

References

1. Analysis of Airborne Particulates and Human Urine by Inductively Coupled Plasma-Atomic Emission Spectrometry, DHHS (NIOSH) Publication No. 79-110.

2. F.N. Abercrombie and R. B. Cruz, Determination of Trace Inorganic Toxic Substances by ICP-AES, Monitoring Toxic Substances, American Chemical Society, February, 1979, pp. 113-135.

3. A. F. Ward, American Laboratory, 10 (1978) 79.

4. P. W. J. M. Boumans and F. J. DeBoer, Spectrochimica Acta, 30B (1975) 309.

5. Jarrell-Ash Div./Fisher Scientific Company, Jarrell-Ash Mark III Atom Comp Interim Operators Manual, Waltham, MA, 1979.

6. L. Ebdon, M. R. Cave and D. J. Mowthorpe, Anal. Chim. Acta., 115 (1980) 179-187.

7. V. A. Fassel and R. N. Kniseley, Anal. Chem., 46 (1974) 1110A.

8. P. W. J. M. Boumans, Optica Pura Y Aplicada, 11 (1978) 143.

9. G. F. Larson, V. A. Fassel, R. H. Scott and R. N. Kniseley, Anal. Chem, 47(1975) 238.

10. R. L. Dahlquist and J. W. Knoll, Applied Spectroscopy 32 (1978) 1.

11. V. A. Fassel, Science, 202 (1978) 183.

12. Botto, R. I. "Interference Correction for Simultaneous Multielement Determinations by Inductively Coupled Plasma," to appear in "Developments In Atomic Plasma Spectrochemical Analysis, Proceedings of the International Winter Conference 1980," Heyden, Philadelphia, 1981.

13. A. F. Ward and H. R. Sobel, ICP Information Newsletter, 3 (1977) pp. 90-112.

14. D. G. Taylor, Manual Coordinator, NIOSH Manual of Analytical Methods - Volumes 1-6, U.S. Government Printing Office, Washington, D.C.

15. R. F. Suddendorf and K. W. Boyer, Anal. Chem., 50 (1978) 1769.

16. M. L. Parsons, A. Forster and D. Anderson, An Atlas of Spectral Interferences in ICP Spectroscopy, Plenum Press, New York, New York, 1980.

17. R. K. Winge, V. J. Peterson and V. A. Fassel, Applied Spectroscopy, 33 (1979) pp. 206-219.

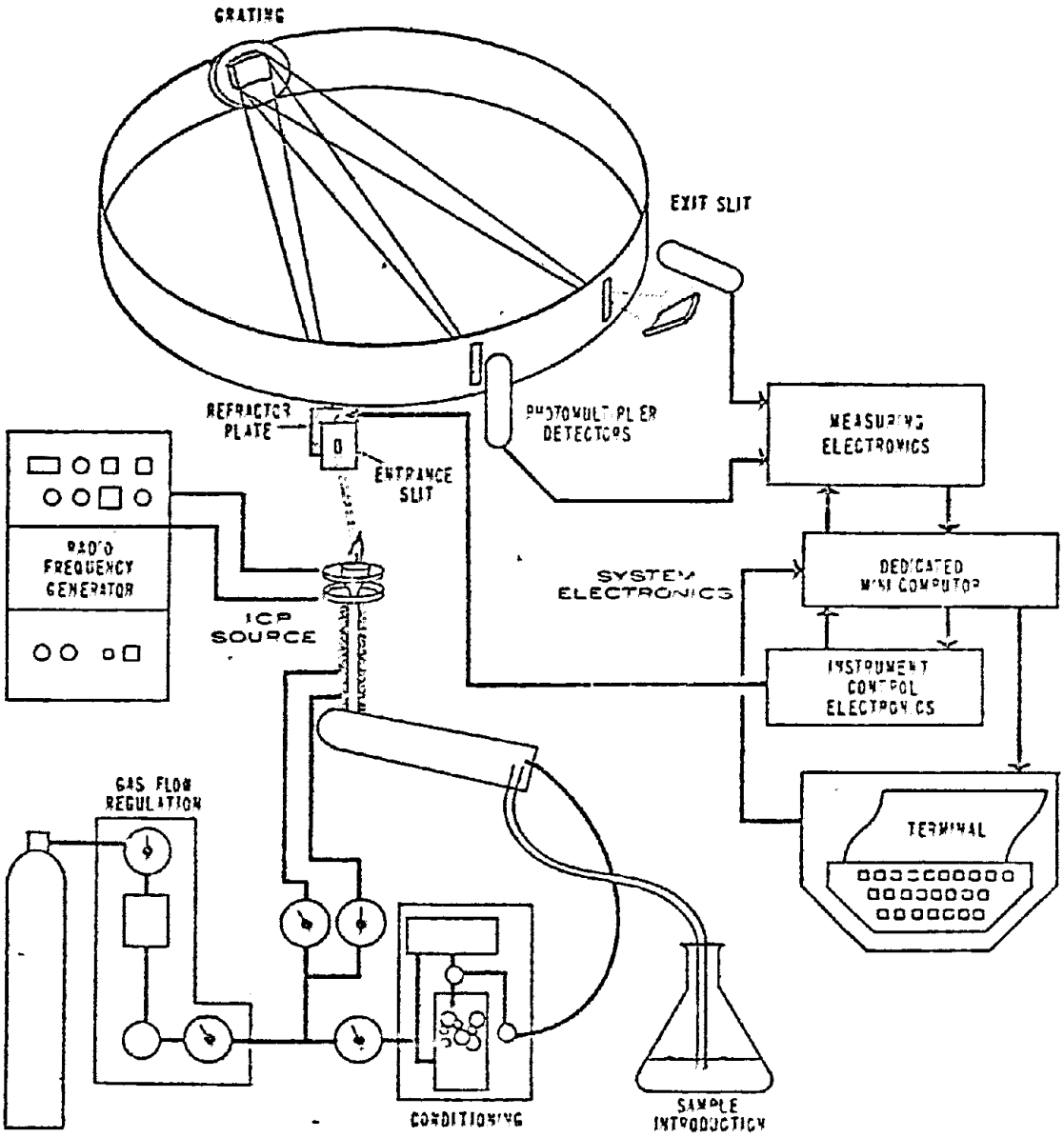

Figure 1. ICP-AES System Schematic

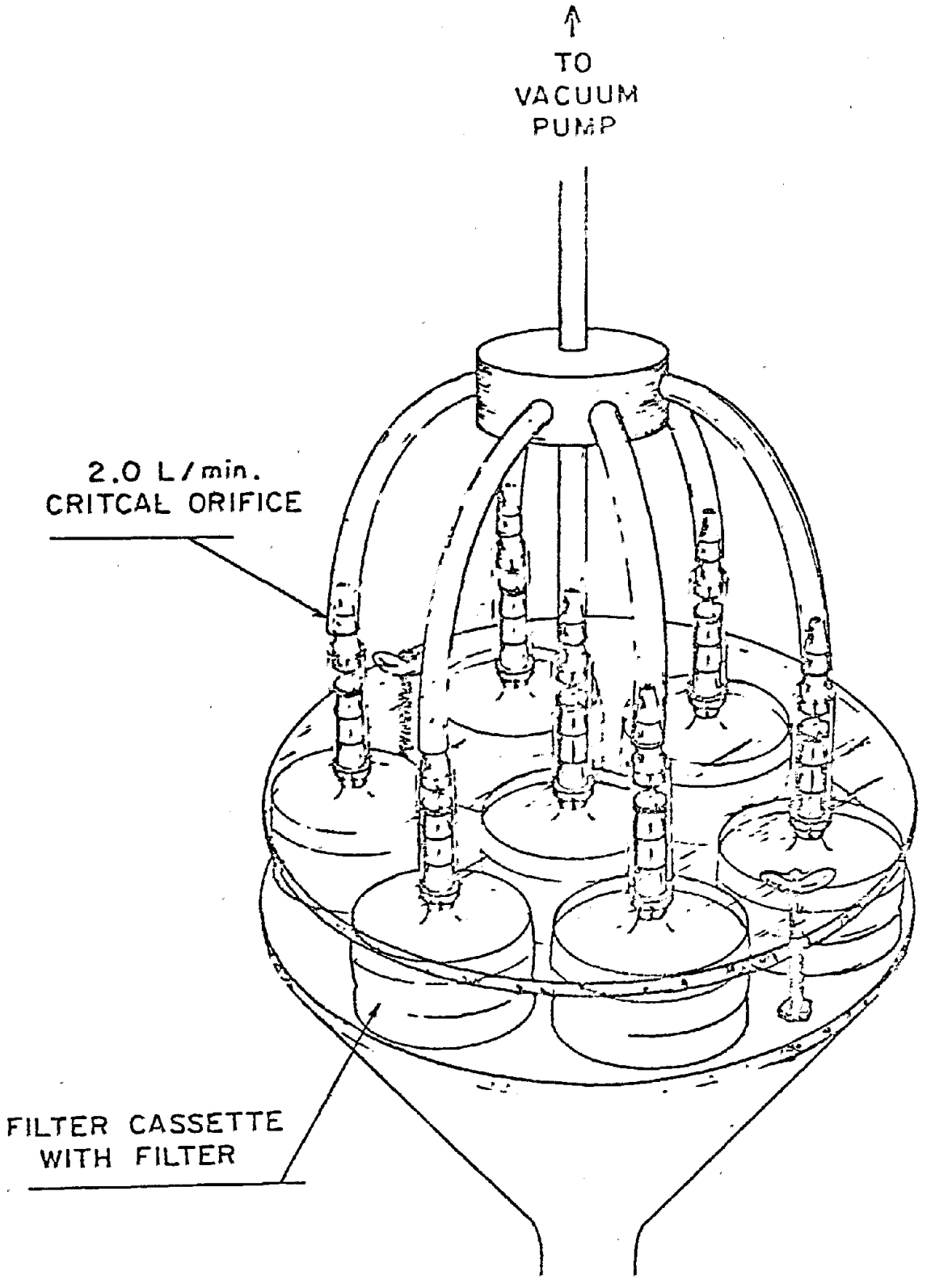

LIPPMAN TYPE SAMPLER

Figure 2.

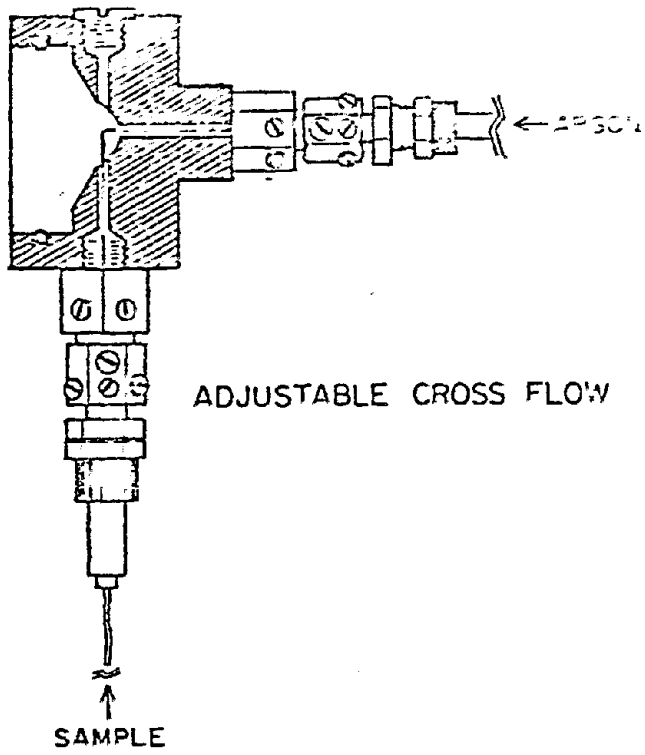

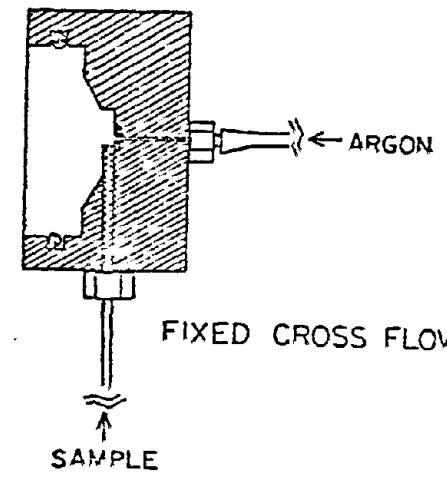

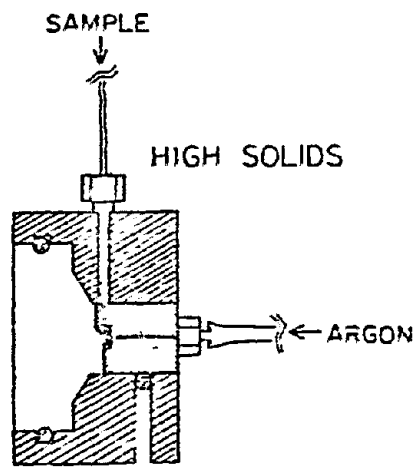

HIGH SOLIDS

Jure 3. Nebulizers

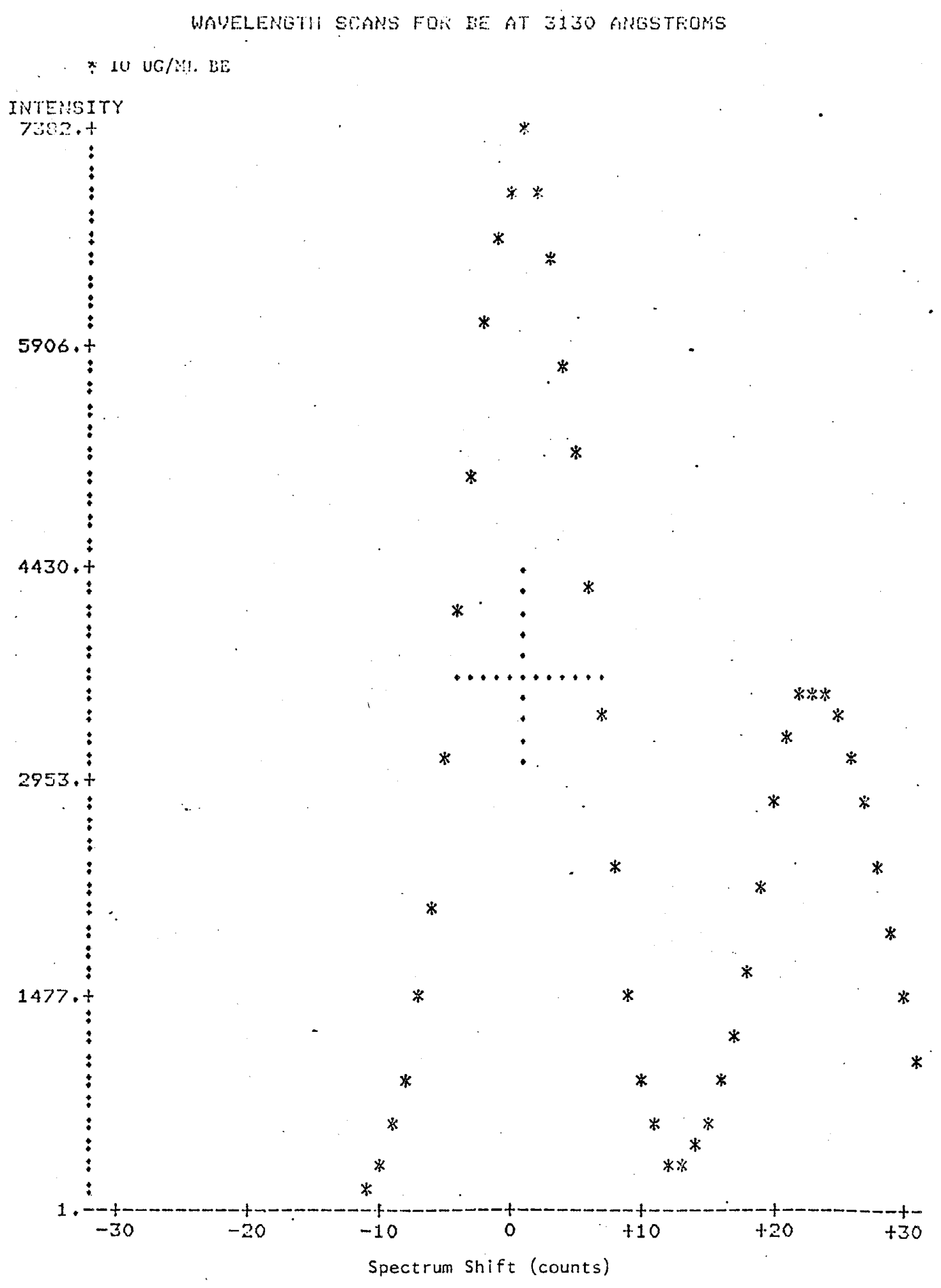

gure 4. Beryllium Scan (peaks at 3130.4A and 3131.1A) 36 36

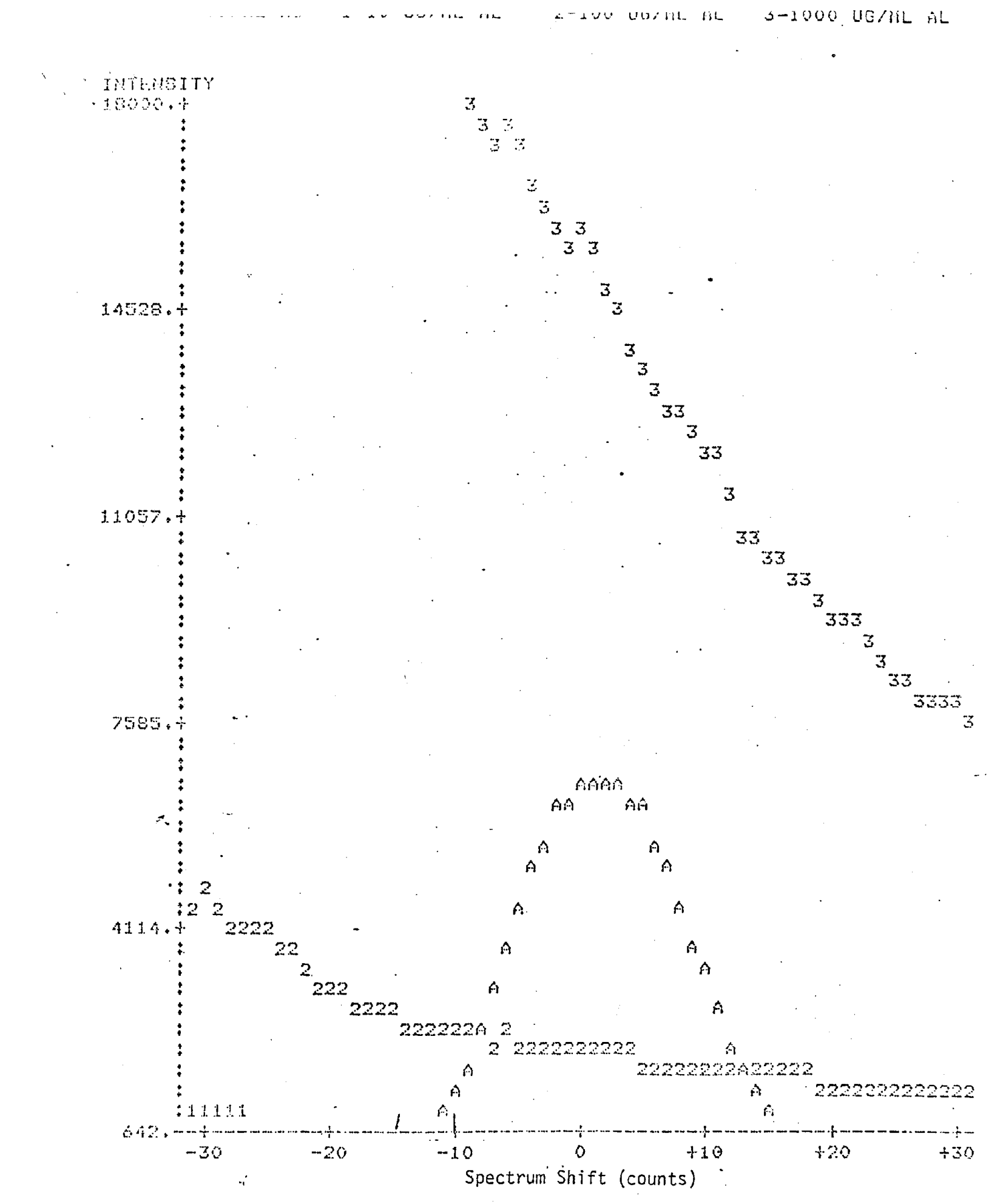

Fig. 5. Elevated background effect of aluminum on arsenic

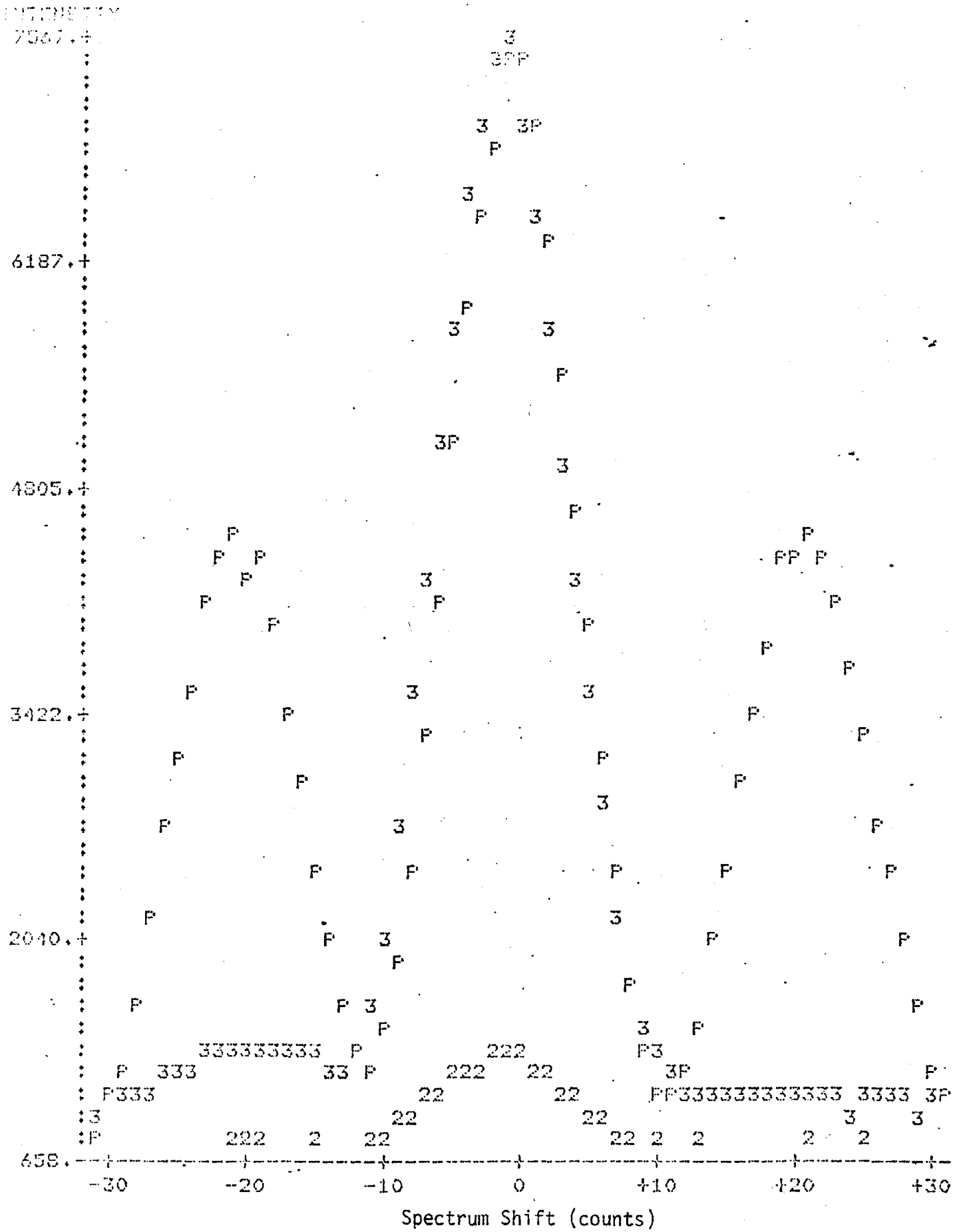

Figure 6. Spectral interference of iron on platinum

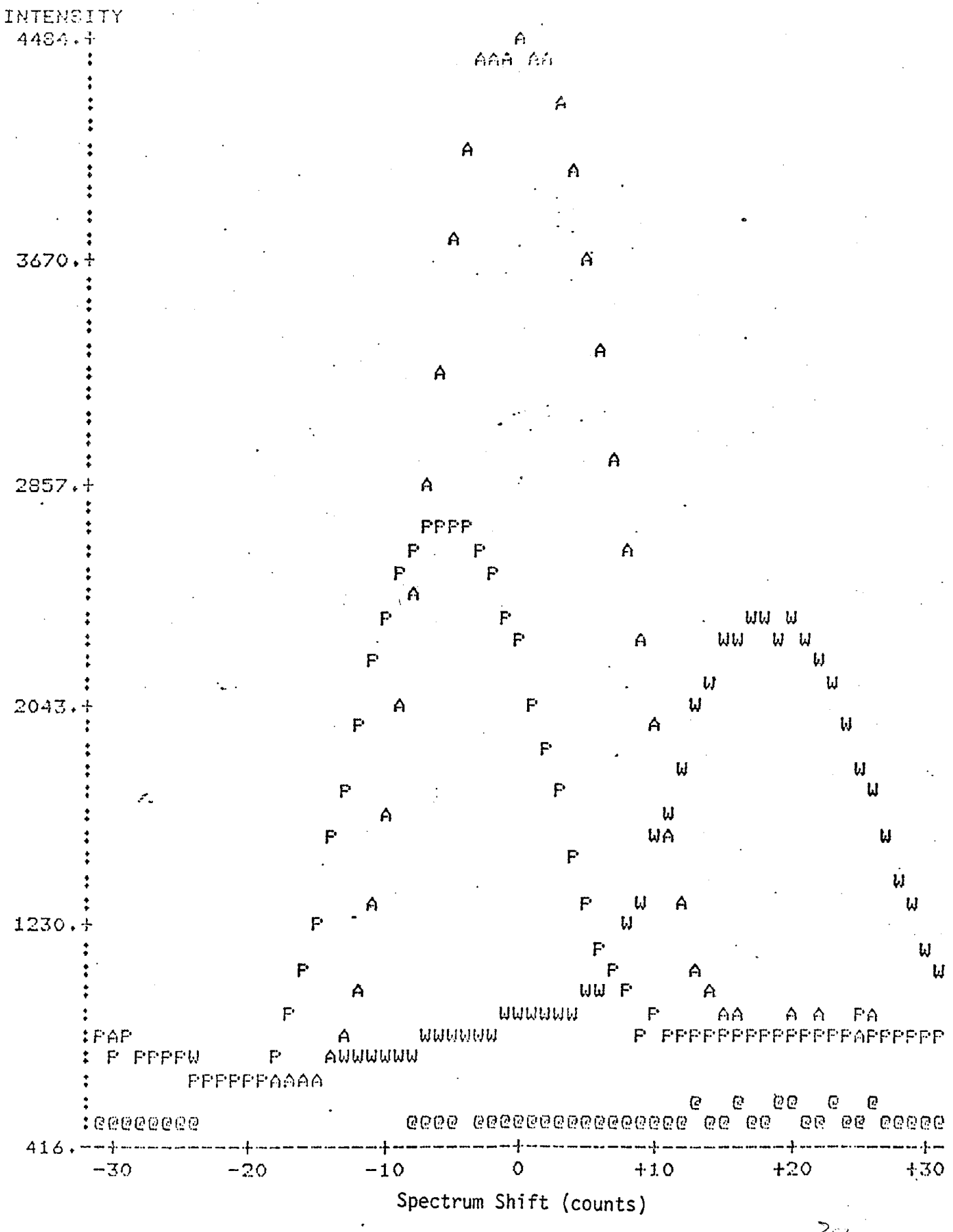

re 7. Spectral interference of platinum and tungsten on arsenic

TABLE I

Occupations With Multielement Exposure

Occupation	Exposure																									
	Al	Ag	As	Ba	Be	B	Cu	Cd	Cr	Co	Fe	Mg	Mn	Mo	Ni	P	Pb	Pt	Se	Te	Tl	Sn	Ti	V	Sb	Zn	Zr
Brass workers			X														X					X				X	
Bronze workers			X				X									X						X			X	X	
Ceramic workers		X	X	X	X					X			X	X	X		X	X		X			X	X	X	X	X
Drug & dye workers		X	X							X		X	X	X	X			X			X	X		X	X	X	
Enamelers			X			X									X		X			X							X
Painters & paint			X	X		X		X					X		X		X						X		X	X	
Textile workers			X	X		X		X	X			X			X				X			X		X	X	X	X
Rubber workers										X									X	X						X	
Glass workers		X		X		X			X	X			X	X			X		X	X	X		X	X			X
Welders							X	X	X		X	X	X													X	
Battery workers							X	X				X	X		X		X										
Solderers		X					X	X									X					X				X	
Electroplaters							X		X	X				X				X								X	
Alloy makers	X	X	X		X	X		X		X		X		X				X		X	X		X	X		X	

Condensed from: Occupational Diseases - A Guide to Their Recognition, U.S. DHEW, pp. 323-412.

TABLE II

Comparison of Trace Metal Techniques

Technique	Initial Cost	No. Samples/Day	No. Elements/Sample	Total No. Elements Determined/Day
Flame AA	15-20K	800-1200*	1	800-1200
Furnace AA	20-30K	50-75*	1	50-75
ICP-AES	75-150K	200-400	10-30	2000-12,000
XRF	80-125K	(~ 2 min/element)		~ 210
XRD	50-90K	15-25	1	15-25

*Considers only one element analyzed for that day. Sample throughput will be less if different elements are determined.

TABLE III

Hardwired Channels

Element	Line Spectrum*	Wavelength (nm)	Element	Line Spectrum*	Wavelength (nm)
Ag	I	328.29	Na	I	589.00
Al	I	308.22	Ni	II	231.60
As	I	193.70	P	I	214.91
B	I	249.68	Pb	II	220.35
Be	II	313.04	Pt	II	203.65
C	I	247.86	Se	I	196.03
Ca	II	315.89	Si	I	288.16
Cd	II	226.50	Sn	II	189.98
Co	II	231.16	Te	I	214.28
Cr	II	205.55	Ti	II	334.94
Cu	I	324.75	Tl	II	190.86
Fe	II	259.94	V	II	310.23
Li	I	670.78	W	II	207.91
Mg	II	279.55	Y	II	371.03
Mn	II	257.61	Zn	I	213.86
Mo	II	281.62	Zr	II	339.20

* I - designates a transition originating from an atomic species.
II - designates a transition originating from an ionic species.

TABLE IV

Technical Specifications

R. F. Generator:	Plasma-Therm, Inc., Model HFS2000D, 27.12 MHz, 2000 watts, crystal controlled.
Induction Coil:	Three and one-half turn, water-cooled, 3.2 mm O.D. copper tubing.
Plasma Torch:	Fused quartz with 3 concentric tube configuration, 20 mm O.D., 1 mm nozzle.
Argon Gas Controls:	Coolant is flow-controlled (0-25 L/min), plasma support argon is flow-controlled (0-5 L/min), aspirator argon is pressure-controlled (0-2 L/min).
Spectrometer:	0.75 meter on Rowland Circle with 2400 grooves/mm (270 nm blaze) grating. Entrance slit height = 3 mm. Entrance slit width - 25 μm. Exit slit width - 50 or 100 μm. Reciprocal linear dispersion - 0.54 nm/mm first order.
Data Handling System:	PDP 11/34 computer and Digital Decwriter II terminal.

TABLE V

Digestion Techniques

Filter Media	Procedure
Cellulose ester	Acid - 12 mL HNO_3 @ 120°C for 24 hrs to near dryness (~ 0.5 mL), cooled, diluted to 5 mL with H_2O. LTA - 6 hrs @ 180 watts and 0.8 torr vacuum, added 0.5 mL HNO_3, heated @ 120°C (15 min) and diluted to 5 mL with H_2O.
PVC co-polymer	Acid - 10 mL HNO_3 + 5 mL $HClO_4$ @ 200°C for 6 hrs, added 10 mL HNO_3 (200°C for 3 hrs), took to near dryness (~ 0.5 mL), diluted to 5 mL with H_2O. LTA - 20 hrs @ 180 watts and 0.8 torr vacuum, added 0.5 mL HNO_3, heated @ 120°C (15 min) and diluted to 5 mL with H_2O.
Polycarbonate	Acid - 5 mL H_2SO_4 @ 120°C for 3.5 hrs, added 0.5 mL H_2O_2, after 1.0 hr added 0.5 mL H_2O_2, took to near dryness (~ 0.5 mL) and diluted to 5 mL with H_2O. LTA - 6 hrs @ 180 watts and 0.8 torr vacuum, added 0.5 mL H_2SO_4, heated @ 120°C (15 min) and diluted to 5 mL with H_2O.

TABLE VI

Optimum Operating Conditions

Nebulizer	Adjustable Cross-Flow (ACF)	Fixed Cross-Flow (FCF)	High Solids (HS)
R. F. Power (K Watts)	0.95	0.95	1.00
Observation Height (mm)	18.0	15.0	17.0
Argon Pressure (nebulizer-psig)	16.0	22.0	27.5
Sample Uptake Rate (mL/min)	0.80	1.45	2.6

TABLE VII

Detection Limits* With Different Nebulizers (ng/mL)

Element	ACF	FCF	HS
Ag	2.0	26.0	6.8
Al	11.8	14.3	36.6
As	18.0	12.7	30.9
B	0.4	1.0	2.8
Be	0.5	1.5	0.4
Ca	7.8	10.4	25.4
Cd	1.7	1.6	2.9
Co	3.7	7.4	18.1
Cr	2.4	1.3	5.2
Cu	1.1	2.1	5.2
Fe	4.9	3.9	8.7
Li	0.7	2.8	4.3
Mg	11.0	23.6	61.2
Mn	0.6	0.4	0.9
Mo	7.0	7.0	15.6
Na	1.4	10.2	20.7
Ni	5.2	3.4	9.0
P	24.6	21.5	44.6
Pb	9.0	16.7	32.6
Pt	12.7	15.4	36.3
Se	19.1	20.9	41.8
Si	5.1	15.8	26.0
Sn	8.9	63.8	23.5
Te	35.2	28.8	118.0
Ti	0.4	1.2	2.8
Tl	24.6	16.9	39.3
V	23.9	3.2	8.7
Y	0.4	0.8	2.0
Zn	1.7	0.6	1.8
Zr	0.9	1.9	5.0

*Two times signal/background ratio.
ACF = Adjustable cross-flow.
FCF = Fixed cross-flow.
HS = High solids.

TABLE VIII

Precision (% RSD)

Element	Short Term Blank Solutions*			Short Term 10.0 µg/mL Standards**			Long Term 10 µg/mL Standards***		
	ACF	FCF	HS	ACF	FCF	HS	ACF	FCF	HS
Ag	1.10	0.87	0.86	0.95	1.36	2.86	1.9	2.7	12.1
Al	0.69	0.46	0.58	0.99	2.17	1.07	2.1	2.5	8.8
As	0.89	0.44	0.64	1.00	0.63	0.54	4.0	3.3	14.2
B	0.58	0.98	1.24	0.63	1.03	0.72	2.4	2.9	14.9
Be	1.12	0.74	0.71	0.68	1.36	1.08	2.6	3.8	10.1
Ca	0.73	0.77	0.82	0.59	1.04	2.22	1.4	4.1	13.1
Cd	1.05	0.88	0.70	1.22	1.06	0.93	3.4	3.9	9.6
Co	0.66	0.81	1.01	1.54	0.95	2.60	2.5	4.1	12.7
Cr	2.06	0.96	1.58	1.07	0.58	2.99	2.4	3.9	9.0
Cu	0.70	0.61	0.72	1.21	1.44	7.79	1.9	2.9	9.2
Fe	1.80	1.02	0.98	1.06	1.06	5.87	2.3	3.5	9.5
Li	1.02	1.10	0.94	2.83	6.02	2.68	1.2	5.3	10.3
Mg	0.90	0.82	1.04	0.50	0.99	0.64	1.9	2.8	13.5
Mn	1.21	0.72	0.70	1.43	1.12	2.51	2.4	3.9	13.2
Mo	1.17	0.91	0.83	0.38	0.75	0.60	2.2	3.2	14.2
Na	0.49	1.14	0.94	2.10	4.60	14.1	5.7	5.2	11.8
Ni	2.28	1.25	1.38	1.01	1.27	1.01	2.8	3.3	9.4
P	1.59	1.24	1.19	0.58	0.99	0.61	3.3	4.1	12.8
Pb	0.55	0.78	0.72	0.66	0.90	2.52	3.3	4.1	12.3
Pt	0.79	0.79	0.76	0.45	1.00	5.92	6.0	4.2	9.4
Se	1.41	1.07	1.11	0.67	0.70	3.09	3.8	3.8	9.6
Si	0.41	0.73	0.66	0.80	1.30	4.59	2.0	2.6	13.1
Sn	1.76	1.22	1.59	0.28	0.69	0.57	3.0	2.8	16.0
Te	0.84	0.65	1.17	0.87	1.12	5.54	3.7	4.3	8.6
Ti	0.46	0.86	0.86	0.55	0.82	3.35	1.7	3.3	8.9
Tl	3.46	2.30	2.04	1.36	1.92	1.43	4.3	3.0	9.4
V	1.27	0.27	0.32	0.75	1.28	2.88	3.3	3.8	13.5
W	0.83	0.86	0.73	0.58	1.15	4.44	3.0	3.5	13.6
Y	0.99	0.85	0.92	0.70	1.22	6.47	1.6	3.1	9.5
Zn	2.95	1.41	2.06	0.61	0.94	2.62	4.2	3.7	12.1
Zr	0.68	0.80	0.84	0.46	0.89	3.16	1.9	2.8	8.9

*Ten 10-second burns.
**Three runs at five 10-second burns/run.
***One 10-second burn every half hour for four hours.

TABLE IX

Nebulizer Comparison

Element	Sensitivity*			Background Equivalent Concentration		
	ACF	FCF	HS	ACF (µg/mL)	FCF (µg/mL)	HS (µg/mL)
Ag	0.393	0.483	0.288	0.179	0.243	0.401
Al	0.137	0.169	0.080	1.41	1.51	3.22
As	0.312	0.490	0.235	1.84	1.13	2.43
B	0.164	0.258	0.133	0.139	0.056	0.120
Be	0.614	1.03	0.506	0.023	0.013	0.029
Ca	0.239	0.376	0.192	0.859	0.822	1.57
Cd	0.428	0.704	0.317	0.137	0.092	0.212
Co	0.293	0.321	0.170	0.350	0.494	0.908
Cr	0.281	0.440	0.201	0.096	0.075	0.168
Cu	0.421	0.456	0.238	0.138	0.195	0.371
Fe	0.078	0.097	0.046	0.194	0.218	0.451
Li	0.212	0.244	0.117	0.079	0.117	0.234
Mg	0.126	0.179	0.085	1.26	1.47	3.00
Mn	0.360	0.542	0.302	0.038	0.033	0.062
Mo	0.092	0.149	0.062	0.454	0.407	0.959
Na	0.309	0.270	0.132	0.426	0.718	1.12
Ni	0.227	0.358	0.156	0.213	0.143	0.336
P	0.085	0.144	0.071	1.41	0.887	1.87
Pb	0.240	0.348	0.185	1.48	1.15	2.29
Pt	0.415	0.531	0.268	1.58	1.10	2.41
Se	0.151	0.254	0.125	1.27	0.938	1.93
Si	0.987	0.415	0.227	0.582	1.11	2.02
Sn	0.241	0.413	0.130	0.400	0.260	0.739
Te	0.023	0.305	0.160	2.59	2.39	5.17
Ti	0.292	0.430	0.191	0.070	0.072	0.164
Tl	0.108	0.167	0.062	0.552	0.374	0.979
V	0.478	0.629	0.339	1.05	0.698	1.39
W	1.55	2.37	0.552	0.668	0.521	2.32
Y	1.26	1.61	0.742	0.039	0.052	0.113
Zn	0.343	0.483	0.318	0.051	0.025	0.045
Zr	0.482	0.692	0.288	0.120	0.127	0.303

ACF = Adjustable cross-flow nebulizer.
FCF = Fixed cross-flow nebulizer.
HS - High solids nebulizer.

* Sensitivity is the slope of the calibration curve (intensity ratio vs. concentration) where the intensity ratio is the absolute intensity of a standard divided by the internal standard (electrical signal for balancing drifts or changes in the electronics) therefore sensitivity units = $\frac{\text{intensity ratio}}{\mu g/mL}$

TABLE X

Calibration in Different Acid Solutions

Element	5% HNO_3			5% HNO_3/5% $HClO_4$			5% H_2SO_4/2% H_2O_2		
	Sensitivity (*)	BEC (µg/mL)	$\bar{S}r$ (%RSD)	Sensivity (*)	BEC (µg/mL)	$\bar{S}r$ (%RSD)	Sensitivity (*)	BEC (µg/mL)	$\bar{S}r$ (%RSD)
Ag	0.610	0.139	0.85	0.592	0.145	0.76	0.537	0.131	1.16
Al	0.182	0.276	0.87	0.176	0.282	0.96	0.160	0.260	0.89
As	0.597	0.623	0.72	0.596	0.638	0.59	0.609	0.604	0.91
B	0.289	0.033	1.22	0.287	0.033	1.17	0.261	0.035	1.13
Be	1.31	0.084	0.56	1.30	0.101	0.96	1.30	0.110	0.71
Ca	0.487	0.336	0.82	0.481	0.348	0.69	0.452	0.319	1.01
Cd	0.918	0.113	0.61	0.905	0.120	0.73	0.825	0.126	0.81
Co	0.415	0.183	0.90	0.409	0.192	0.48	0.380	0.182	0.94
Cr	0.530	0.063	1.32	0.525	0.073	1.21	0.494	0.065	1.42
Cu	0.584	0.123	1.34	0.584	0.126	1.39	0.539	0.117	1.39
Fe	0.108	0.027	0.97	0.108	0.027	0.76	0.101	0.026	0.77
Li	0.159	0.026	2.63	0.147	0.033	3.48	0.143	0.031	3.29
Mg	0.224	0.294	1.06	0.221	0.296	0.83	0.184	0.243	0.98
Mn	0.727	0.044	0.58	0.719	0.050	0.70	0.674	0.046	1.00
Mo	0.179	0.073	0.81	0.179	0.074	0.75	0.169	0.072	1.01
Na	0.205	0.148	2.34	0.195	0.156	2.04	0.183	0.159	2.60
Ni	0.423	0.068	1.01	0.413	0.074	0.89	0.385	0.076	0.58
P	0.187	0.385	1.83	0.186	0.394	2.30	0.196	0.369	2.47
Pb	0.451	0.570	0.80	0.451	0.485	0.61	0.400	0.460	0.84
Pt	0.725	0.732	0.82	0.722	0.743	0.87	0.666	0.697	0.73
Se	0.322	0.282	0.96	0.320	0.295	0.82	0.472	0.286	1.38
Si	0.485	0.542	0.98	0.498	0.555	1.25	0.453	0.514	1.76
Sn	0.313	0.072	0.89	0.312	0.074	0.99	0.282	0.143	0.83
Te	0.413	0.802	0.70	0.411	0.817	0.67	0.457	0.777	0.83
Ti	0.517	0.049	1.19	0.511	0.054	0.95	0.487	0.054	1.26
Tl	0.144	0.053	1.69	0.414	0.055	1.08	0.129	0.059	1.15
V	0.822	0.472	0.57	0.807	0.482	0.48	0.764	0.457	0.74
W	2.71	1.59	1.37	2.94	1.63	0.93	2.79	1.54	1.13
Y	2.01	0.178	1.06	2.01	0.170	1.11	1.90	0.163	1.32
Zn	0.658	0.042	0.76	0.646	0.047	1.56	0.580	0.042	1.13
Zr	0.836	0.136	1.17	0.827	0.146	0.89	0.789	0.149	1.52

Sensitivity = slope of calibration curve.

BEC = background equivalent concentration (intercept of calibration curve).

$\bar{S}_r$ = pooled relative standard deviation.

$* = \frac{\text{intensity ratio}}{\mu g/mL}$

TABLE XI

Effect of Peristaltic Pump

Element	Without Pump				With Pump			
	Acid Blank Intensity (counts)	Net* Intensity (counts)	Precision** (% RSD)	Detection Limit (Absolute Intensity)	Acid Blank Intensity (counts)	Net* Intensity (counts)	Precision** (% RSD)	Detection Limit (Absolute Intensity)
Ag	975.0	49,970	0.36	19.3	880.6	52,583	0.67	40.4
Al	2,156.0	14,667	0.80	31.7	2,084.0	16,995	2.14	64.1
As	4,711.0	46,783	1.46	89.8	4,843.0	49,754	0.38	140.3
B	176.2	25,090	2.63	6.07	165.6	27,955	0.61	15.1
Be	119.0	43,627	0.86	0.0002	130.0		0.81	0.0001
Ca	2,524.0	35,264	0.25	35.6	2,326.0	35,867	0.28	87.8
Cd	543.0	61,753	0.61	14.0	529.6	65,626	0.54	19.5
Co	1,316.0	29,834	0.34	19.3	1,224.0	30.740	0.16	44.1
Cr	280.6	40,608	1.10	14.5	268.6	43,884	0.43	12.7
Cu	761.6	47,926	1.23	15.3	720.2	54,458	0.88	2.22
Fe	181.4	9,392	0.60	3.90	169.8	10,127	0.43	6.23
Li	240.0	17,951	2.37	2.45	217.0	28,969	9.84	9.17
Mg	2,183.0	16,828	1.70	45.2	2,028.0	18,596	0.51	90.6
Mn	155.2	55,983	0.34	2.19	147.0	58,481	0.25	6.0
Mo	505.0	12,839	1.55	15.2	481.8	13,854	0.30	17.3
Na	1,628.0	24,747	3.31	9.63	1,253.0	33,775	2.73	24.7
Ni	403.6	30,315	0.65	20.9	401.8	32,989	0.58	0.63
P	1,095.0	13,533	1.78	48.5	1,099.0	14,406	0.66	4.37
Pb	3,399.0	33,606	0.31	67.7	3,341.0	34,225	0.19	144.0
Pt	4,995.0	54,889	0.59	88.3	5,165.0	58,756	0.45	135.8
Se	2,054.0	24,062	0.85	61.9	2,067.0	26,133	0.83	83.9
Si	4,108.0	38,655	0.93	79.6	3,795.0	42,218	0.82	249.4
Sn	823.2	24,647	1.27	18.7	841.6	25,444	0.57	34.1
Te	5,981.0	33,315	0.43	44.1	6,335.0	35,280	0.42	147.4
Ti	264.8	38,428	1.52	5.90	242.6	43,195	0.82	9.34
Tl	515.8	12,353	1.17	12.3	510.6	13,920	1.37	27.7
V	3,581.0	62,146	0.37	16.3	4,059.0	66,482	0.49	32.4
W	10,790.0	69,259	0.94	261.0	10,599.0	79,973	0.58	404.5
Y	721.8	#	0.84	12.8	646.8	#	0.60	28.7
Zn	110.0	53,638	0.16	4.69	115.6	55,312	0.39	3.35
Zr	744.0	58,710	1.44	13.5	685.6	65,713	0.74	23.2

*Intensity difference between 10 µg/mL standard and acid blank.
**Precision is of three 10-second burns of a 10 µg/mL standard.
#Off scale.

TABLE XII

Effect of Nebulizer Argon Humidification

Element	With Humidification				Without Humidification			
	5% HNO_3 Blank		10 µg/mL Standard		5% HNO_3 Blank		10 µg/mL Standard	
	Intensity (counts)	Precision (% RSD)	Intensity (counts)	Precision (% RSD)	Intensity (counts)	Precision (% RSD)	Intensity (counts)	Precision (% RSD)
Al	2,394.0	1.44	19,078	1.13	3,021.0	0.74	19,032	1.48
Cd	615.5	1.98	74,261	0.55	807.6	1.01	85,603	1.14
Li	260.3	1.61	20,671	4.98	330.3	0.93	15,497	4.67
Ni	455.0	2.33	36,051	0.58	592.2	1.24	39,270	1.33
Tl	607.3	2.58	16,356	1.17	748.7	1.98	17,562	1.75

All intensity determinations are the average of five 10-second burns replicated three times. The precision reported is the pooled value from the burns.

TABLE XIII

Interference Effects Produced by High Salt Content

	Absolute Intensity				
Without Humidification	Al	Cd	Li	Ni	Tl
5% HNO_3	19,032 (1.48)	85,603 (1.14)	15,497 (4.67)	39,270 (1.33)	17,562 (1.75)
5% HNO_3 + 1% NaCl	17,886 (1.46)	81,234 (1.27)	13,937 (3.17)	36,591 (1.35)	16,200 (1.57)
5% HNO_3 + 5% NaCl	16,967 (1.60)	73,314 (1.88)	17,791 (3.00)	32,645 (1.76)	14,494 (2.16)
5% HNO_3 + 10% NaCl	16,592 (1.65)	68,981 (2.12)	21,969 (3.31)	30,392 (1.96)	13,613 (1.86)
With Humidification					
5% HNO_3	19,078 (1.13)	74,261 (0.55)	20,671 (4.98)	36,051 (0.58)	16,356 (1.17)
5% HNO_3 + 1% NaCl	17,758 (0.89)	71,073 (0.53)	16,517 (2.42)	33,569 (0.57)	14,890 (0.66)
5% HNO_3 + 5% NaCl	16,846 (0.97)	66,052 (0.78)	18,982 (1.86)	30,443 (0.75)	13,537 (1.17)
5% HNO_3 + 10% NaCl	16,606 (1.03)	60,025 (0.77)	23,389 (1.53)	27,754 (0.77)	12,390 (1.06)

Analysis consisted of five 10-second burns triplicated.

TABLE XIV

Interferences

Element Aspirated (100 ppm)	Channels Giving Response																												
	Ag	Al	As	B	Be	Ca	Cd	Co	Cr	Cu	Fe	Li	Mg	Mn	Mo	Na	Ni	P	Pb	Pt	Se	Si	Sn	Te	Ti	Tl	V	W	Y	Zn	Zr
Ag																															
Al			EB												CO			EB	EB	EB	EB		EB	EB		EB		EB			
As																															
B			EB																									EB			
Be			EB	CO		EB			II												EB					EB	EB				
Ca																CO															
Cd																CO		EB						EB							
Co			II			CO	II										II		II	II	II					II					
Cr			EB			EB									II	CO				EB											
Cu																		II	EB	II				EB				II		II	
Fe			II	CO				II												II	II					EB					
Li																															
Mg															EB																
Mn											II		II		II											II					
Mo		CO	EB			II		EB	EB	CO	CO		II					EB	EB	II	II			II		II		II			
Na																						CO									
Ni							II	II	II										EB											CO	
P																															
Pb			EB																							EB					
Pt			II													CO								II							
Se																															
Si																CO															
Sn																CO															
Te						CO																									CO
Ti	II	II				EB				II	II					CO							II	EB		II					
Tl																															
V		II	II		II	II					CO													II		II					
W		CO	II	CO		EB		II	II		II		EB			CO		II	II	II	CO		II	II		II					
Y	II	EB				CO																									
Zn																		EB						EB					II		
Zr	EB				II	II							II														EB				
1000 ppm																															
Na																						CO									
K			EB			CO							CO		EB	CO		EB				CO		EB							

II - Interelement Interference
EB - Elevated Background
CO - Contamination

TABLE XV

Interelement Corrections

Affected Channel	Affecting Element	K*	Affected Channel	Affecting Element	K*
Ag	Zr	0.0060	Pb	W	0.0042
Al	Ti	0.0037	Pt	Al	0.0044
Al	V	0.0273	Pt	Co	0.0589
As	Al	0.0310	Pt	Cu	0.0027
As	Fe	0.0044	Pt	Fe	0.0072
As	Mo	0.0025	Pt	Mo	0.0058
As	Pt	0.5107	Pt	W	0.0049
As	V	0.0263	Se	Al	0.0048
As	W	0.0195	Se	W	0.0106
Be	V	0.0065	Sn	Ti	0.0039
Ca	Be	0.0034	Te	Al	0.0027
Ca	Mo	0.0042	Te	Cd	0.0551
Ca	Ti	0.0026	Te	Cu	0.0027
Ca	W	0.0026	Te	Mo	0.0059
Ca	Zr	0.0039	Te	Pt	0.0072
Cr	Be	0.0011	Te	V	0.1271
Fe	Mn	0.0028	Te	W	0.0079
Mg	Mn	0.0028	Te	Zn	0.0160
Mo	Mg	0.0205	Tl	Co	0.0036
P	Al	0.0027	Tl	Ti	0.0064
P	Cd	0.0027	Tl	V	0.0022
P	Cu	0.0150	Tl	W	0.0056
P	Mo	0.0056	W	Al	0.0033
P	W	0.0256	W	Zn	0.0191
Pb	Co	0.0026	Zn	Cu	0.0025
Pb	Ni	0.0030			

*K = Interelement correction factor.

TABLE XVI

Typical Calibration Curve Parameters

Element	Intercept (µg/mL)	Slope*
Ag	0.14975	0.65419
Al	1.00790	0.23389
As	0.89850	0.57159
B	0.04323	0.33396
Be	0.01105	1.28844
Ca	0.53498	0.49386
Cd	0.07097	0.82666
Co	0.35944	0.37792
Cr	0.05632	0.50369
Cu	0.10697	0.72336
Fe	0.14512	0.13242
Li	0.4787	0.48007
Mg	1.00652	0.22451
Mn	0.2165	0.73723
Mo	0.29761	0.18381
Na	0.19261	0.75806
P	0.68499	0.17115
Pb	0.84186	0.42478
Pt	0.75712	0.69068
Se	0.76176	0.27677
Si	0.75648	0.54496
Sn	0.22071	0.49201
Te	1.61171	0.41199
Ti	0.04839	0.54522
Tl	0.26719	0.22414
V	0.53566	0.87838
W	0.41111	2.58342
Y	0.03030	2.34908
Zn	0.02091	0.60304
Zr	0.08636	0.87599

$* = \frac{\text{intensity ratio}}{\mu g/mL}$

TABLE XVII

Quantitative Limits and Precision

Element	Calculated Detection Limit (ng/mL)	Lower Quantitative Limit for Analysis (ng/mL)	$\bar{S}_r$* at Lower Limit (%RSD)	$\bar{S}_r$* at 10-µg/mL (% RSD)	Stability** (%)
Ag	2.0	50	0.35	0.95	-1.2
Al	14.0	50	0.38	0.99	-1.3
As	15.0	100	0.53	1.00	+2.7
B	2.0	10	1.41	0.63	+0.1
Be	0.2	10	0.45	0.68	-0.1
C		Not Quantitative		17.4	+42.0
Ca	11.0	50	0.56	0.59	-0.6
Cd	2.0	10	0.46	1.22	-3.8
Co	6.0	50	0.53	1.54	-1.8
Cr	3.0	10	1.27	1.07	-0.4
Cu	1.0	10	0.27	1.21	-2.4
Fe	3.0	50	0.59	1.06	-2.2
Li	1.0	10	0.63	2.83	+1.8
Mg	22.0	50	0.69	0.50	+1.0
Mn	0.5	10	0.32	1.43	+2.2
Mo	6.0	50	0.49	0.38	-0.5
Na	5.0	50	0.79	2.10	-5.3
Ni	5.0	50	0.64	1.01	-4.2
P	46.0	100	0.85	0.58	+0.6
Pb	15.0	100	0.55	0.66	+0.9
Pt	16.0	100	0.65	0.45	-0.2
Se	36.0	100	1.74	0.67	-1.1
Si	4.0	50	0.46	0.80	+1.6
Sn	11.0	100	1.24	0.28	+0.7
Te	29.0	100	0.77	0.87	+2.6
Ti	0.9	10	0.32	0.55	+0.7
Tl	21.0	50	1.56	1.36	-0.2
V	3.0	10	0.27	0.75	+0.1
W	13.0	50	0.70	0.58	-1.8
Y	0.7	50	0.26	0.70	-2.3
Zn	1.0	10	1.31	0.61	+0.02
Zr	2.0	50	0.36	0.46	-0.9

$$*\bar{S}_r^2 = \frac{(n-1)S^2 + (n-1)S_2^2 + (n-1)S_3^2}{n + n_2 + n_3 - 3} = \frac{S_1^2 + S_2^2 + S_3^2}{3}$$

(Three runs at 5 burns/run.)

**Stability = change in response for 10 µg/mL solution over a four-hour period.

TABLE XVIII

Multielement Standards

Standard	Elements
1	None (Blank solution)
2	Ag, Ca, Co, Mn, Pb, V, Zn
3	Al, Be, Cd, Li, Ni, Tl
4	As, B, Mg, Mo, P, Sn
5	Cu, Fe, Na, Pt, Te, Y
6	Si, W
7	Cr, Se, Ti, Zr

TABLE XIX

Variable Wavelength Channel (N + 1)

Element (Analyte)	λ (nm)	Slits Ent. (μ)	Slits Exit (μ)	Aperture (mm)	Dynode (gain)	Detection Limit (μg/mL)	Lower Quant. Limit (ppb) (μg/mL)	$\bar{S}_r$* @ Lower Limit (%)	$\bar{S}_r$* @ 10 μg/mL (%)	Stability** (%)	Interferences***
Ba	455.4	10	20	6	1.0	~1	50	0.67	1.22	+0.8	None
Hf	277.3	30	40	8	5.0	13	50	0.63	0.55	-0.8	Fe, Pt, Zr: Elevated background
Rh	233.5	50	50	10	7.0	50	500	0.45	0.34	+0.8	Fe, Mg: Elevated background
Sb	206.8	35	40	8	8.7	13	100	0.38	0.73	-0.1	Co (Sb λ = 231.147)
Ta	226.2	30	40	8	7.0	23	250	0.45	0.44	-2.5	Fe (Ta λ = 260.349); Ni, Se, W: Elevated background

*Pooled relative standard deviation (3 runs @ 5 burns/run).
**Change in response for 10 ppm solution over a 2-3 hour period.
***Elements which show a bias when the analyte is aspirated.

TABLE XX

Metals in Cellulose Ester Filters (µg/filter)

Element	Detection Limit (µg/filter)	Lot #31076-4		Lot #C7M21891		Lot # 080577A05	Lot # 080577A06
		LTA	HNO_3	LTA	HNO_3	HNO_3	HNO_3
Ag	0.008	--	--	--	--	--	--
Al	0.04	--	--	0.04	0.22	0.13	0.46
As	0.04	--	--	--	--	--	--
Be	0.0008	--	--	--	--	--	--
Ca	0.03	2.9	3.1	2.5	3.0	1.1	0.97
Cd	0.004	--	--	--	--	--	--
Co	0.02	--	--	--	--	--	--
Cr	0.004	0.40	0.44	0.24	0.25	1.2	1.3
Cu	0.008	0.11	0.12	0.29	0.29	0.046	0.047
Fe	0.008	0.067	0.052	0.079	0.071	0.150	0.20
Li	0.008	--	--	--	--	--	--
Mg	0.03	0.57	0.64	0.46	0.47	0.17	0.17
Mn	0.003	0.009	0.010	0.017	0.018	0.006	0.006
Mo	0.03	--	--	--	--	--	--
Na	0.04	5.0	6.7	7.9	8.1	2.7	4.3
Ni	0.004	0.005	0.006	0.005	0.006	0.006	0.006
P	0.04	0.65	0.68	3.8	2.4	2.3	2.2
Pb	0.04	--	--	--	--	--	--
Pt	0.04	--	--	--	--	--	--
Se	0.04	--	--	--	--	--	--
Sn	0.03	--	--	--	--	--	--
Te	0.08	--	--	--	--	--	--
Ti	0.005	--	--	--	--	--	--
Tl	0.02	--	--	--	--	--	--
V	0.04	--	--	--	--	--	--
W	0.08	--	--	--	--	--	--
Y	0.003	--	--	--	--	--	--
Zn	0.002	0.11	0.11	0.058	0.045	0.055	0.074
Zr	0.008	--	--	--	--	--	--

TABLE XXI

Metals in Filters (μg/filter)

	PVC copolymer				Polycarbonate			
	Lot #81867		Lot #2595099		Lot #73B8345		Lot #81F7A37	
Element	LTA	$HNO_3/HClO_4$	LTA	$HNO_3/HClO_4$	LTA	H_2SO_4/H_2O_2	LTA	H_2SO_4/H_2O_2
Ag	--	--	--	--	--	--	--	--
Al	0.13	--	0.15	--	--	--	--	--
As	--	--	--	--	--	--	--	--
Be	--	--	--	--	--	--	--	--
Ca	13.3	12.2	4.6	4.0	0.05	--	0.16	--
Cd	0.041	--	0.114	0.094	--	--	--	--
Co	--	--	--	--	--	--	--	--
Cr	0.65	0.89	0.27	0.35	0.27	0.27	--	--
Cu	0.22	0.14	0.22	0.15	--	--	0.024	--
Fe	0.10	*	0.11	*	--	--	--	--
Li	--	--	--	--	--	--	--	--
Mg	0.34	0.21	9.0	8.4	--	--	--	--
Mn	0.016	--	0.020	--	--	--	--	--
Mo	--	--	0.20	0.18	--	--	--	--
Na	35.1	19.3	28.3	24.0	--	--	--	--
Ni	--	--	--	--	--	--	--	--
P	0.48	0.41	0.06	0.02	0.06	--	--	0.07
Pb	0.18	--	0.24	--	--	--	--	--
Pt	--	--	--	--	--	--	--	--
Se	--	--	--	--	--	--	--	--
Sn	--	--	--	--	--	--	--	--
Te	--	--	--	--	--	--	--	--
Ti	--	--	--	--	--	--	--	--
Tl	--	--	--	--	--	--	--	--
V	--	--	--	--	--	--	--	--
W	--	--	--	--	--	--	--	--
Y	--	--	--	--	--	--	--	--
Zn	0.086	0.22	0.061	0.19	0.006	0.005	0.003	--
Zr	--	--	--	--	--	--	--	--

*Very high blanks ($\bar{X}$ = 2.4 μg/mL).

TABLE XXII

Reagent Blanks Comparison
(µg/mL)

Element	LTA HNO_3	Ultrapure HNO_3 Lot A	Ultrapure HNO_3 Lot B	ACS Reagent HNO_3
Al	--	0.54	0.51	0.89
Ca	--	0.13	0.07	3.0
Cr	--	0.005	--	0.12
Cu	--	--	--	0.022
Fe	0.011	0.131	0.081	0.45
Mg	--	--	--	0.11
Mn	--	--	--	0.009
Na	0.48	5.2	5.2	9.52
Ti	--	0.007	0.007	0.012
Zn	--	0.022	0.013	0.023
Zr	--	0.044	0.044	0.050

TABLE XXIII

Recoveries from Spiked Filters*

Element	2.5 µg/Filter		1000 µg/Filter	
	HNO_3 Recovery (%)	$HNO_3/HClO_4$ Recovery (%)	HNO_3 Recovery (%)	$HNO_3/HClO_4$ Recovery (%)
Ag	93	111	97	91
Al	100	93	101	100
As	112	103	96	99
Be	100	107	93	90
Ca	104	99	100	95
Cd	100	107	105	99
Co	101	101	95	95
Cr	93	98	103	106
Cu	99	98	96	99
Fe	100	94	100	97
Li	97	89	92	95
Mg	96	105	106	106
Mn	103	84	78	93
Mo	94	94	85	88
Na	**	**	97	101
Ni	95	105	103	97
P	**	**	81	91
Pb	99	105	98	95
Se	73	105	89	97
Sn	7.1	74	45	67
Te	90	102	102	94
Ti	83	96	15	108
Tl	96	103	105	99
V	96	99	95	94
W	64	35	32	23
Y	101	99	101	100
Zn	101	101	96	94
Zr	83	4.9	100	98

*N = 3 for each case.
**Blank levels too high to make accurate determination.

TABLE XXIV

Welding and Brazing Samples*
(µg metal/filter)

Stainless Steel-Stick

Loading	Iron		Nickel		Chromium		Manganese	
	ICP	AAS	ICP	AAS	ICP	AAS	ICP	AAS
A	8.9	7.0	2.8	1.6	6.4	5.8	3.6	3.2
B	16.2	14.5	4.5	3.8	12.3	12.1	7.5	7.3
C	36.2	36.4	10.7	11.9	27.5	28.5	17.4	18.2
D	57.6	58.0	16.5	17.8	43.7	43.7	28.2	28.6
E	104.0	103.0	30.9	33.4	75.9	72.7	48.6	47.7

Stainless Steel - MIG

Loading	Iron		Nickel		Chromium		Manganese	
	ICP	AAS	ICP	AAS	ICP	AAS	ICP	AAS
A	8.5	7.6	2.4	1.5	4.8	3.3	2.4	1.2
B	12.2	11.6	4.0	3.7	6.8	5.5	3.3	3.0
C	57.1	59.5	21.8	23.4	32.1	32.9	13.8	14.3
D	79.6	81.2	28.7	31.4	42.8	43.3	28.1	29.7

Mild Steel - Braze

Loading	Zinc		Cadmium		Silver	
	ICP	AAS	ICP	AAS	ICP	AAS
A	9.4	10.3	23.5	13.3	0.54	**
B	80.6	87.7	168	185	2.1	1.1
C	101	107	260	286	2.5	1.6
D	183	193	422	440	3.5	1.9

*N = 5 filters for each case.
**Concentration less than detection limit.

TABLE XXV

Alloying Plant Samples

	Acid Digestion		Low Temperature Ashing	
	ICP-AES µg/filter	AAS µg/filter	ICP-AES µg/filter	AAS µg/filter
Nickel				
Sampler I	264	263	137	135
	191	167	178	169
	240	238		
$\bar{X}$	232	223	158	152
Sampler II	146	151	127	122
	181	184	89.5	94.2
			135	129
$\bar{X}$	164	168	117	115
QA* (% Recovery)	(103)	(108)	(99.5)	(102)
Iron				
Sampler I	8.29	8.27	3.60	4.32
	5.45	5.15	4.23	4.11
	8.31	8.49		
$\bar{X}$	7.35	7.30	3.92	4.22
Sampler II	7.26	7.38	4.14	3.64
	7.98	8.18	2.79	3.50
			4.08	3.31
$\bar{X}$	7.62	7.78	3.67	3.48
QA (% Recovery)	(112)	(102)	(100)	(96.2)
Copper				
Sampler I	122	122	82.9	78.1
	76.0	72.9	101	94.5
	107	102		
$\bar{X}$	102	99.0	92.0	86.3
Sampler II	65.9	63.4	72.8	69.0
	64.9	64.7	48.3	46.2
			68.2	65.5
$\bar{X}$	65.4	64.1	63.1	60.2
QA (% Recovery)	(102)	(111)	(108)	(111)

*QA = Quality assurance spikes (N = 3).

TABLE XXVI

Metals Determined by ICP-AES (μg/filter)

Metal	Al	Ca	Cr	Mg	Mn	Ti
Low Temperature Ashing:						
Sampler I	8.8	19.7	0.91	1.97	2.66	3.49
	9.1	19.0	0.90	2.20	2.89	3.90
Sampler II	9.0	22.2	1.35	2.00	2.53	3.57
	6.6	18.7	0.86	1.60	1.95	2.69
	9.4	21.3	1.89	1.45	2.92	4.15
Filter Blanks	--*	5.7	0.14	0.72	--	--
	--	4.9	0.15	0.77	--	--
	--	7.6	0.17	1.63	--	--
Acid Ashing:						
Sampler I	16.6	28.2	3.43	3.40	4.83	7.00
	11.9	20.1	2.61	2.87	3.75	5.65
	13.5	22.9	1.34	3.56	3.78	5.67
Sampler II	11.8	27.0	2.85	3.48	2.64	4.16
	13.1	26.3	3.61	3.33	3.17	4.82
Filter Blanks	4.6	10.0	0.29	1.94	--	--
	4.4	11.5	0.23	2.73	0.10	--
	3.0	7.1	0.22	1.72	--	--

*Less than 0.1 μg/filter.

TABLE XXVII

Plating Plant Samples

	$HNO_3/HClO_4$ Ash			HNO_3 Ash	
	ICP-AES (µg/filter)	AAS (µg/filter)		ICP-AES (µg/filter)	AAS (µg/filter)
Chromium					
Sample			Sample		
2	1.88	2.17	1	2.73	2.91
4	2.40	2.63	3	2.04	2.66
6	2.39	*	5	1.41	1.77
			7	3.86	3.71
$\bar{X}$	2.22	2.40		2.51	2.69
QA**(30 µg)	(105)	(104)		(98.4)	(97.0)
QA (150 µg)	(102)	(95.7)		(99.2)	(93.2)
Nickel					
Sample			Sample		
2	9.32	9.32	1	12.2	13.4
4	14.4	14.1	3	11.9	12.2
6	13.0	13.4	5	8.57	8.37
			7	17.1	17.0
$\bar{X}$	12.2	12.3		12.4	12.7
QA (25 µg)	(101)	(114)		(101)	(104)
QA (100 µg)	(101)	(102)		(100)	(93.8)

*Sample lost.
**QA = Quality assurance samples (% recovery for 3 spiked filters).